THE HYDROCHEMISTRY AND AGE OF THE WATER IN THE MILK RIVER AQUIFER, ALBERTA, CANADA

by

Gerald Bernard Swanick

A Thesis Submitted to the Faculty of the

DEPARTMENT OF HYDROLOGY AND WATER RESOURCES

In Partial Fulfillment of the Requirements
For the Degree of

MASTER OF SCIENCE
WITH A MAJOR IN HYDROLOGY

In the Graduate College

THE UNIVERSITY OF ARIZONA

1 9 8 2

STATEMENT BY AUTHOR

This thesis has been submitted in partial fulfillment of requirements for an advanced degree at The University of Arizona and is deposited in the University Library to be made available to borrowers under rules of the Library.

Brief quotations from this thesis are allowable without special permission, provided that accurate acknowledgment of source is made. Requests for permission for extended quotations from or reproduction of this manuscript in whole or in part may be granted by the head of the major department or the Dean of the Graduate School when in his judgment the proposed use of the material is in the interests of scholarship. In all other instances, however, permission must be obtained from the author.

SIGNED: Gerald B. Swanick

APPROVAL BY THESIS DIRECTOR

This thesis has been approved on the date shown below:

S. N. Davis

S. N. DAVIS
Professor of Hydrology
and Water Resources

May 21, 1982
Date

ACKNOWLEDGMENTS

The author is sincerely grateful to Dr. Stanley N. Davis for his thoughtful guidance during this undertaking. Many thanks are due to Dr. Harold Bentley for the thought-provoking discussions and his suggestions to new approaches. Drs. L. Graham Wilson and Austin Long were helpful in their discussion as the work progressed. Thanks are also expressed to Mr. James Brinkman, who wrote the computer program used in the hydrodynamic age dating. The patience and support of Ms. Deborah Flower were elemental in the progress of this work.

The work was supported by the Battelle Project Management Division, Office of Nuclear Waste Isolation, Columbus, Ohio, on Contract #E512-04900-1.

TABLE OF CONTENTS

TABLE OF CONTENTS--Continued

LIST OF ILLUSTRATIONS

LIST OF ILLUSTRATIONS--Continued

LIST OF TABLES

ABSTRACT

The Milk River aquifer system in Alberta, Canada, was studied to develop age-dating techniques for old ground water. A steady-state flow model used to calculate hydrodynamic ages of the ground water and ^{14}C concentrations in the water were used to calculate ages for comparison. The results were compared with ^{36}Cl-predicted ages of the same aquifer. The ages predicted with the flow model showed a progression of increasing age from zero at the Milk River sandstone outcrop near the United States–Canadian border to 500,000 years near Taber, a town about 60 miles northwest of the outcrop. A sensitivity analysis on the input parameters to the flow model indicated that the predicted age of the water is most sensitive to changes in sandstone porosity and the vertical permeability of the shales and clays overlying and underlying the sandstone aquifer.

INTRODUCTION

The purpose of this project was to estimate the age of the water in the Milk River sandstone in southeastern Alberta, Canada. For this thesis, the term "age" is defined as the length of time a particle of water has been separated from exposure to the atmosphere. Usually that length of time can be considered the time since the water moved below the root zone of plants and into the saturated subsurface. By knowing the age of ground water, the direction and speed of migration of the water can be determined. Dating of ground water is one way to determine the suitability of a given rock unit for an underground repository for hazardous wastes. The direction of movement of ground water and the time required to move a given distance can be used to predict the potential spread of water-borne contaminants.

To verify the predicted age by any method, the age of the ground water must be estimated by alternate means. In a fairly simple flow system, conventional hydraulic calculations can be used to estimate the ages. These results can be compared to ages predicted from the decay of radioactive nuclides in the water. This latter method requires an extensive understanding of the flow system and the ion geochemistry of the ground water of concern. The Milk River sandstone aquifer in southeastern Alberta is a likely candidate for age dating because of its limited extent and because it has been extensively studied and described.

This study was based on available data from published and unpublished sources and the chemical data collected from the study area by Thomas LaMarche and me for The University of Arizona during the summers of 1979 and 1980. Geologic and hydrologic data were used in the model WADAMO, a quasi-three-dimensional, steady-state flow model developed by James Brinkman at The University of Arizona in 1980 to predict ground-water ages based on the hydrodynamics of the aquifer. Carbonate and carbon-isotope data were used in models proposed by Tamers (1975) and Fontes and Garnier (1979) to determine the ground-water ages.

Previous Studies

The major contribution to the understanding of geology and structure in northern Montana was published by Kemp and Billingsley in 1921. These investigators described the general petrology and the structural and stratigraphic relations of the intrusive Sweet Grass Hills and the surrounding sedimentary rocks. The most complete study of the geology of southwestern Alberta was done by Russell and Landes (1940). Their work was based on work by previous investigators and on field studies done from 1931 to 1937. They described the formations with much detailed stratigraphy. Crockford (1949) made a substantial contribution to the understanding of the origin, physical characteristics, and stratigraphy of the units overlying the Milk River Sandstone.

The major work responsible for the interpretation of the ground-water hydrology of southern Alberta was reported by Meyboom (1960). This work was followed by the report of Borneuf (1976) in

which he described the hydrogeology of the eastern half of the study area of this thesis.

Analysis and interpretation of the geochemistry of the groundwater in the Milk River sandstone was first made by Meyboom (1960), later by Borneuf (1976), and most recently by Schwartz and Muehlenbachs (1979, 1980). In these two works, Schwartz and Muehlenbachs analyzed the stable isotope and hydrochemistry of the Milk River sandstone aquifer and postulated several hypotheses for the chemical patterns they found.

Location and Physiography of the Study Area

The area under investigation includes the southeastern corner of Alberta and a small section of north-central Montana (fig. 1). It is bounded on the south by the Sweet Grass Hills in Montana, on the east by the 110° longitude, on the west by the 112°30' longitude, and on the north by the 50° latitude.

The area is bordered in the east by the Cypress Hills, which rise to 4,700 feet, to the west by the Milk River Ridge, which rises to 4,100 feet, and to the south by the Sweet Grass Hills, which rise to 4,200 feet above mean sea level. The intervening plain is a gently rolling terrain, which slopes from 3,000 feet in the south and west to 2,500 feet in the north and east. The plain is cut by several large gullies, called coulees, and several streams, which flow eastward from the Milk River Ridge and westwestward from the Cypress Hills. Figure 2 shows the major geographic features in the study area.

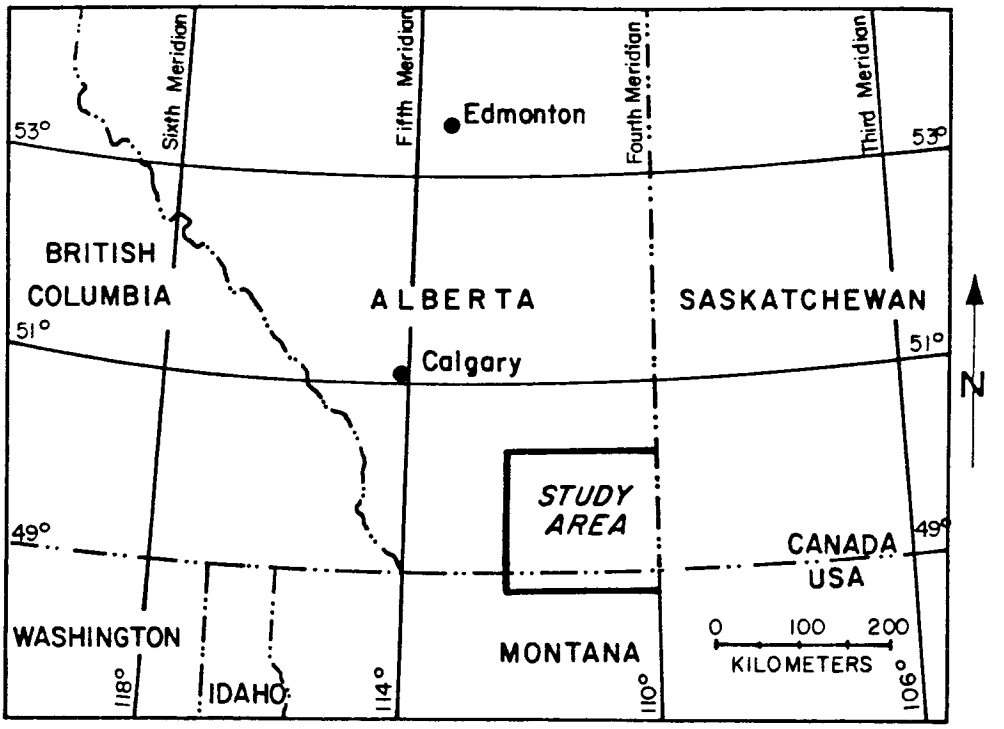

Figure 1. Location of the study area

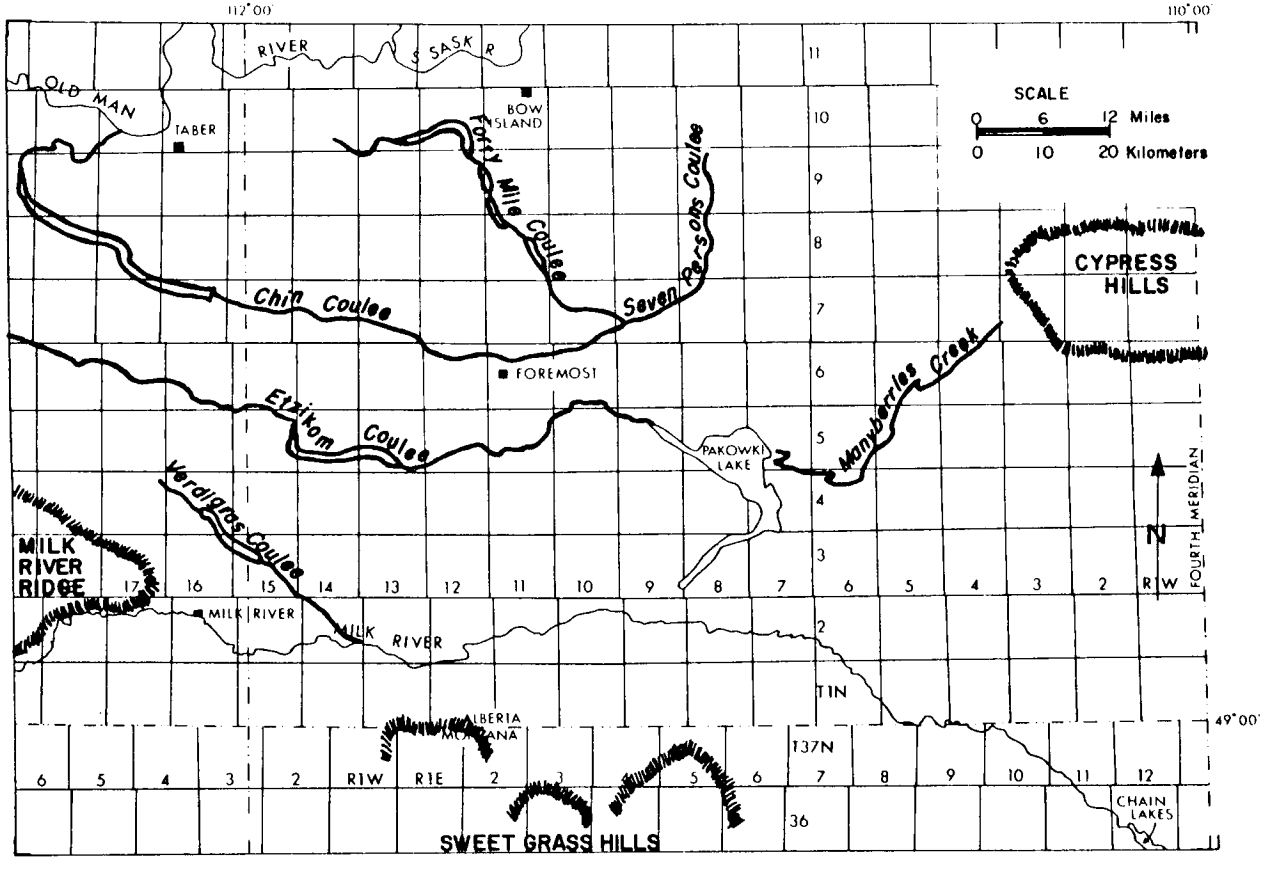

Figure 2. Major geographic features in the study area

The South Saskatchewan River system drains the northern reaches of the study area, including the northern slopes of the Cypress Hills. This system flows generally eastward and has a maximum mean discharge of 7,500 cubic feet per second (cfs) at Medicine Hat. The Milk River drains the southern part of the study area and the southern slopes of the Cypress Hills. This river flows eastward across the study area just north of the international boundary and has a mean discharge of about 300 cfs. Situated between the South Saskatchewan River and Milk River systems is Pakowki Lake, a closed internal drainage basin. Streams and creeks that drain into Pakowki Lake are generally small, the largest being Manyberries Creek, which has a mean discharge of about 14 cfs.

Climate and Vegetation

Except for the Cypress Hills, the climate is cold and semiarid, with a mean annual temperature of 43°F and a mean annual precipitation of 13 inches. The Cypress Hills have a precipitation in excess of 16 inches (Borneuf, 1976).

Most of the land area is used for agriculture, mainly wheat and barley. Prairie grasses and sagebrush are the dominant vegetation in the nonagricultural parts of the study area. Some coulees and rivers are lined with trees, and the Cypress Hills are forested on their northern slopes with lodgepole pine, aspen, poplar, and spruce.

GEOLOGY

Southern Alberta is underlain by rocks mainly of Cretaceous age, which consist of a series of interbedded sandstones and shales (fig. 3). The Lower Cretaceous strata consist principally of green and reddish shales with one or more zones of sandstone or sandy shale (Russell and Landes, 1940). These strata are overlain by the Colorado formation, a thick shale sequence containing several sandstone beds, which in turn is overlain by the Milk River formation and a succession of sandstone and shale units. A description of the Colorado formation upward should provide an understanding of the location, extent, and stratigraphy of the Milk River sandstone.

The Colorado formation comprises about 1,700 feet of shale with several "salt-and-pepper" sandstone units. Meyboom (1960) described four such sandstone units in ascending order.

1. Basal Colorado sandstone: a fine- to medium-grained sandstone interbedded with silty shale, approximately 10 feet thick, which lies at the base of the formation.

2. Bow Island sandstone: a series of fine-grained sandstones, approximately 75 feet thick, which are commonly topped by a pebble bed. The Bow Island sandstone is the producing zone of several gas fields in southern Alberta.

3. Fish Scale sandstone: a sandstone, only a few feet thick, which is considered to be the top of the Lower Cretaceous strata.

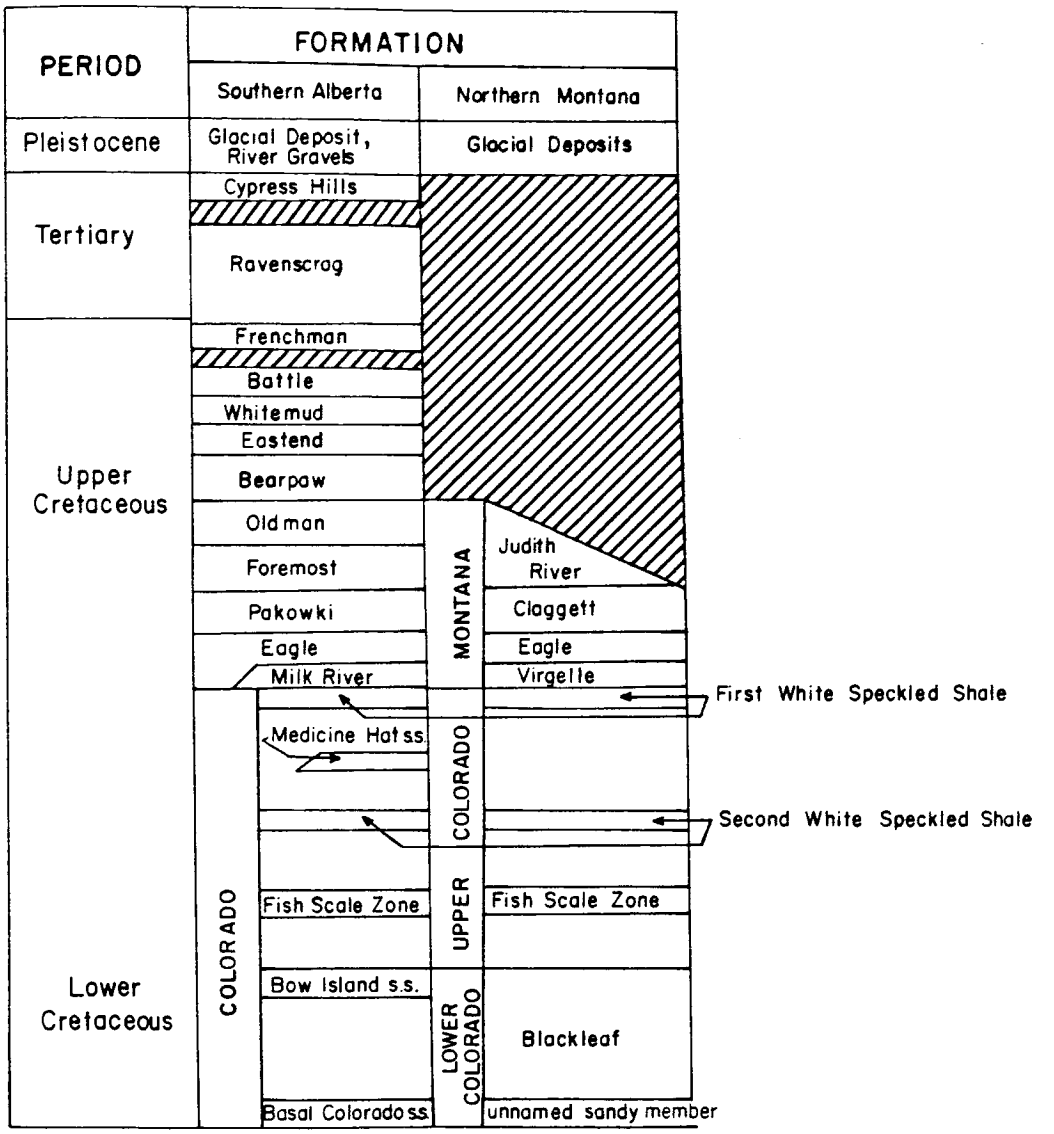

Figure 3. Stratigraphic column for southern Alberta and northern Montana

4. Medicine Hat sandstone: a fine- to medium-grained sandstone, which lies about 100 feet below the top of the formation. It is the producing zone of the Medicine Hat gas field. Williams and Burk (1964) described the Medicine Hat as lenses of sandstone, up to 45 feet thick, whose individual bodies appear to be discontinuous and completely enclosed in shale.

The upper part of the Colorado formation comprises beds of fairly uniform, dark-gray shales with occasional concretions and bentonite beds. The 50-foot interval above the Colorado formation grades from shales into sandy shales and eventually into the sandstone of the Eagle formation, which is in the stratigraphic interval between the top of the Colorado formation and the base of the Pakowki formation. Where present, the Milk River sandstone is the basal member of this formation.

The typical Milk River sandstone beds consist of massive, medium-grained sandstone with concretions, grading downward into shaly sandstone and sandy shale. These beds are exposed at land surface along the Milk River mostly around Ts. 1 and 2, Rs. 11 through 16 west of the fourth meridian (fig. 4) and in the Sweet Grass Hills in northern Montana as encircling rims around three buttes (Kemp and Billingsley, 1921). The sandstone dips to the north, east, and west of the outcrop area in the Sweet Grass Hills.

The unnamed nonmarine, upper member of the Eagle formation is commonly composed of argillaceous sandstones and sandy clays with

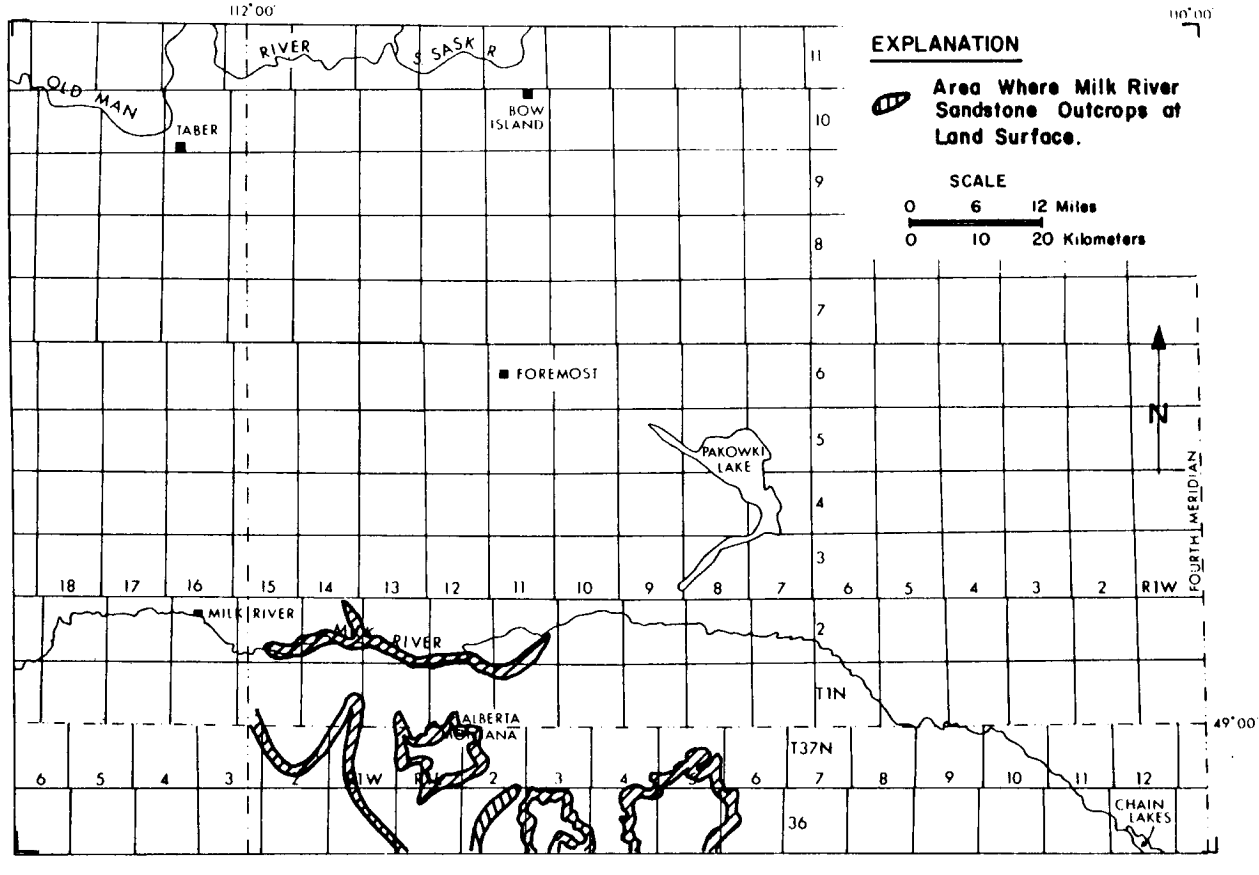

Figure 4. Areas of outcrop of the Milk River sandstone at land surface

some lenticular beds of massive, light-buff sandstones. Streaks of lignite of up to 0.5 foot in thickness are common.

Both the upper and lower members of the Eagle formation gradually thin toward the north and east and thicken toward the west. In the northeastern corner of the area, the sandstone wedges out and the formation is represented by marine beds, mostly shale, which are usually included as part of the younger Pakowki formation (Russell and Landes, 1940).

The Pakowki formation directly overlies the Eagle formation where it is present and is in direct contact with the Colorado formation shales where the Eagle is missing. The Pakowki formation consists of marine shales with thin layers of ironstone, silty shale, and bentonite. The contact between the Pakowki formation and older beds is easily recognized by the 0.5- to 1-foot-thick chert pebble bed that is the lowermost part of the Pakowki. The thickness of the Pakowki formation in the study area ranges from more than 150 feet in the southwest to 900 feet in the northeast. The position of the top of the formation is sometimes difficult to determine because of the similarities between its shales and those of the lower beds of the overlying Foremost formation.

The lithology of the Foremost formation is highly variable but is generally gray and dark-gray shales, coal seams, thin sandstone beds, and some shell-bearing beds (brackish-water molluscs). This formation ranges in thickness from about 100 to 200 feet throughout the study area and is overlain by the Oldman formation.

Rocks typical of the Oldman formation are sandstones and soft, plastic shales. Beds of ironstone or indurated sandstone are common but discontinuous, and coal seams are common in the upper part of the formation. The thickness ranges from 200 to 600 feet.

The Bearpaw formation is composed almost exclusively of shales of marine origin. Thin beds of bentonite and fine-grained clayey sandstone of great lateral extent are common throughout.

The uppermost Cretaceous strata are evident in the highland areas adjacent to the plains. The Bearpaw formation in the Cypress Hills is overlain by a series of shale, sandstone, bentonite, and coal beds, and the flanks of the Milk River Ridge are overlain by stratigraphically equivalent beds. Except in the Cypress Hills, many hundreds of feet of Tertiary and Cretaceous sediments were eroded from the area during the early Quaternary and Tertiary (Taylor, Mathews, and Kupsch, 1964). Pleistocene glacial drift of varying thickness covers most of the area; on the north side of the Cypress Hills, the upper limit of the glacial deposits is at approximately 4,000 feet (Gravenor and Bayrock, 1965).

A structure map (fig. 5) of the top of the Milk River sandstone reveals a radiating pattern of closely connected folds. In the western part of the study area, the fold axes are generally to the west and northwest, and in the eastern part most axes trend east and northeast. The Sweet Grass Hill intrusions, produced by plutonic activity during the Eocene (Taylor and others, 1964), probably along with more deeply seated intrusions, disturbed the regional dip in the area and caused the

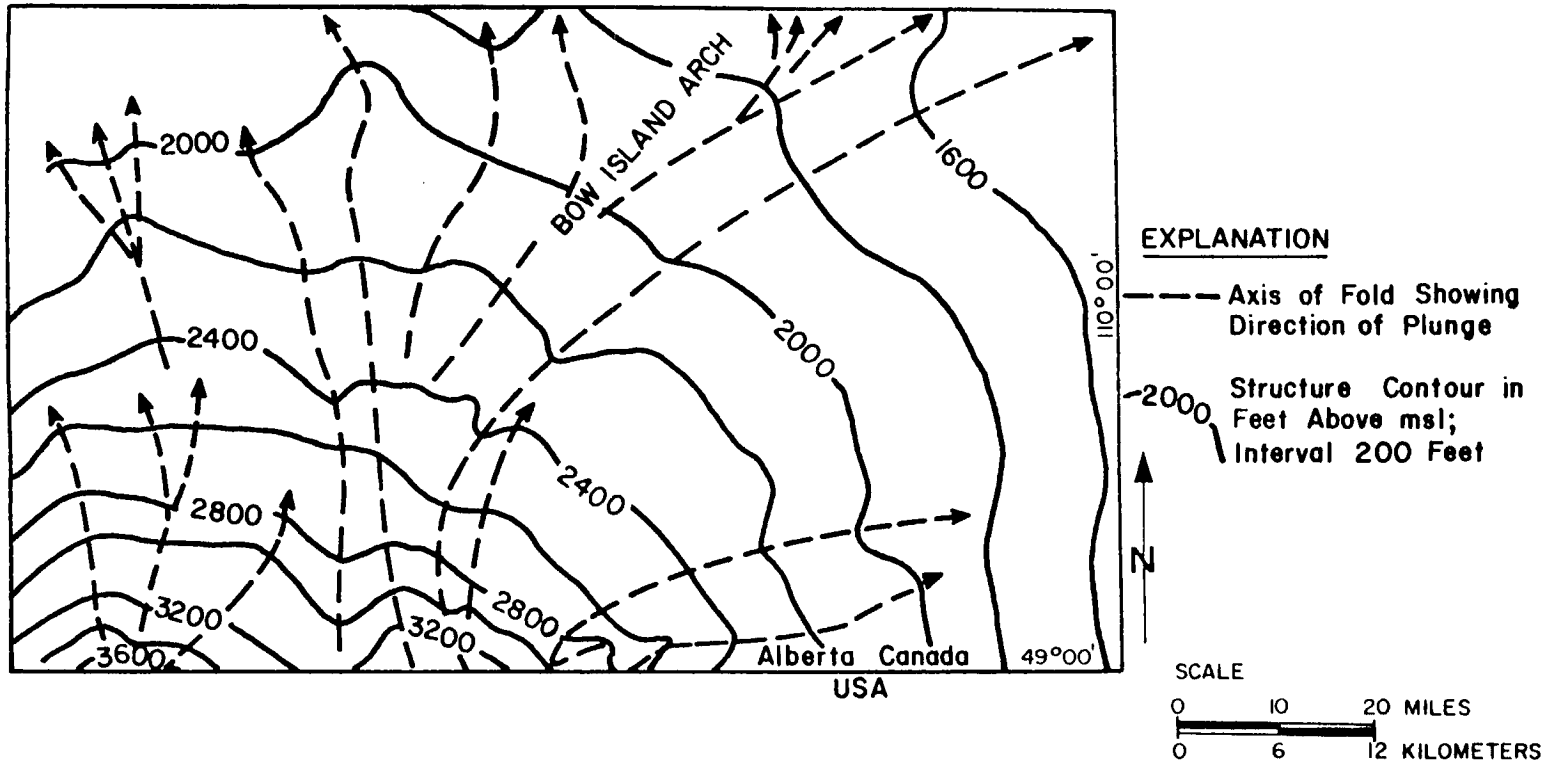

Figure 5. Structure contours on the Milk River sandstone. -- After Meyboom (1960)

fanlike structural pattern of the Milk River sandstone from Montana into Alberta.

HYDROLOGY

The ground-water system in the study area comprises three main water-bearing strata: the glacial drift, which covers the land surface over most of the area; the Milk River sandstone, which crops out along the flanks of the Sweet Grass Hills and dips north below the study area; and the Bow Island sandstone, which crops out south of the study area, also dips north, and is about 1,200 to 1,400 feet below the Milk River sandstone. These aquifers are separated by confining beds comprised of the shales and clays of the intervening formations. Figure 6 shows a typical cross section of the Milk River sandstone aquifer.

Most of the area is covered by glacial drift of varying thickness, except for the Cypress Hills, which were not affected by glacial activity, and the coulees from which the drift cover has been removed. In the eastern part of the study area, the glacial drift is the main aquifer used for water supply. The water table is within 50 feet of land surface over most of the area and is nearer land surface in the eastern part. Figure 7 shows the water-table elevations within the study area.

The Milk River sandstone forms an artesian aquifer over a large part of southern Alberta and a small part of northern Montana. The Milk River aquifer had no water-well development until 1916, but in 1937 there were 250 wells and in 1960 there were 409 water wells producing from it (Meyboom, 1960). Of the 409 wells, just less than

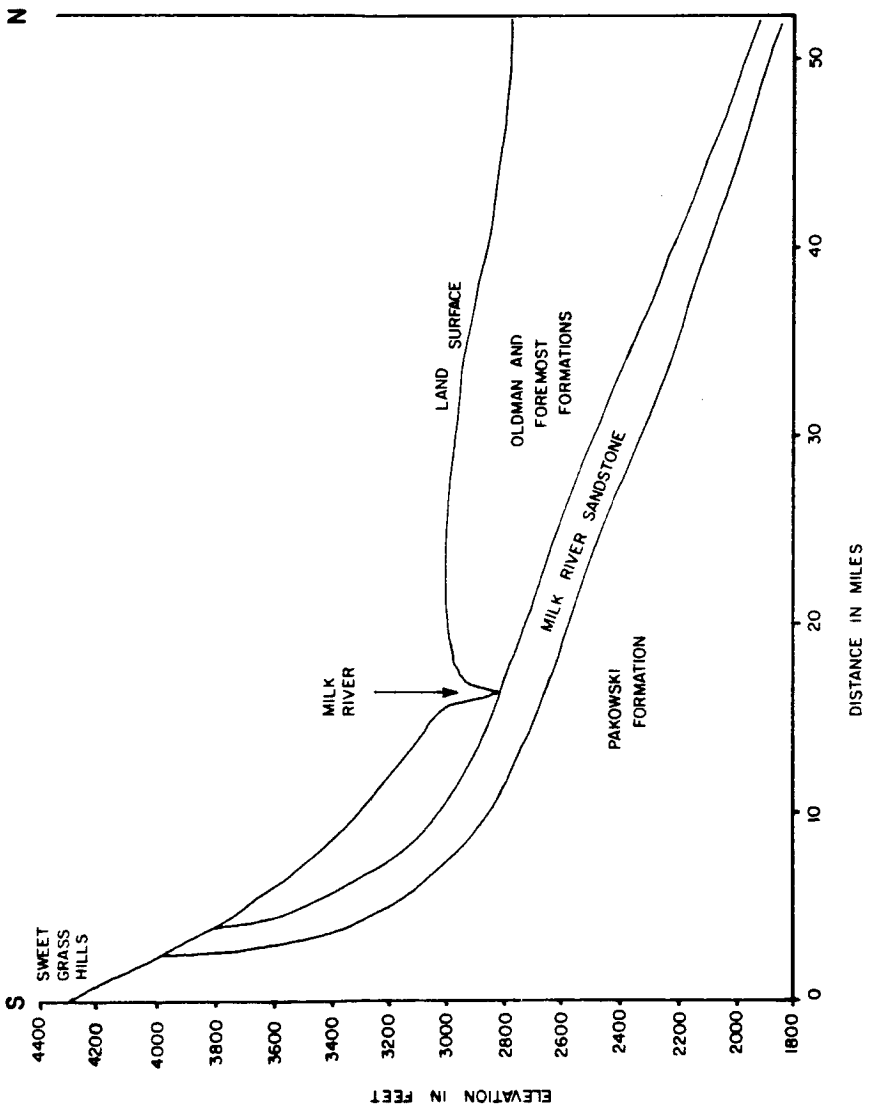

Figure 6. A typical cross section of the Milk River sandstone aquifer

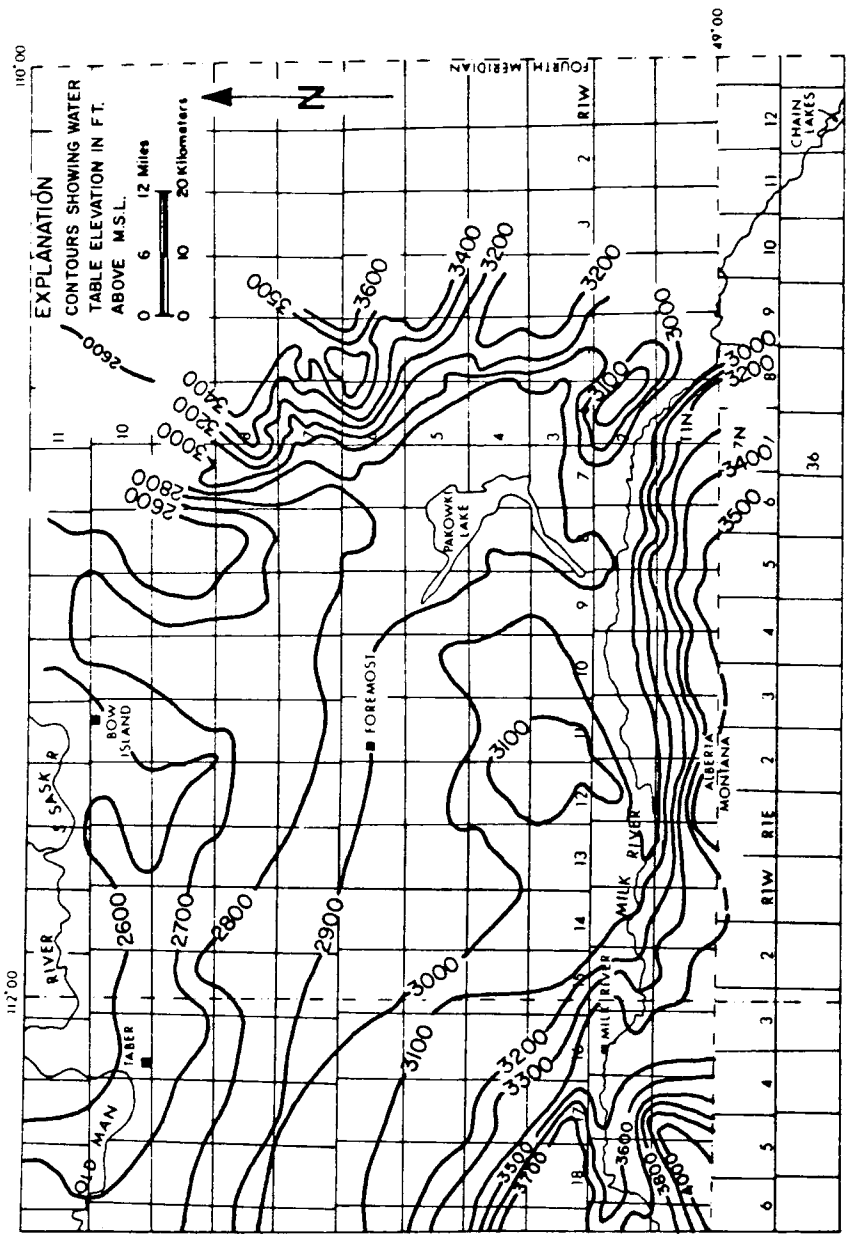

Figure 7. Contours of the water table in the surficial deposits

half were flowing in 1960. Most wells tapping the Milk River aquifer are in the central part of the study area. Total ground-water production was estimated to be 700,000 gallons daily in 1960.

The potentiometric surface of the Milk River aquifer in 1958 is shown in figure 8. Prior to water-well development of the aquifer, the potentiometric surface would have been controlled by the rates of recharge and natural recharge and the thickness and permeability of the sandstone. The original gradient was probably toward the north, east, and west. Because of the present ground-water extraction, the gradient is now steepened in the north and reversed in the east and west (Meyboom, 1960).

The hydraulic system was also disturbed by postglacial downcutting of the Milk River valley into the Milk River Sandstone (Meyboom, 1960). Surface exposures of the sandstone can be seen along the Milk River in Ts. 1 and 2, Rs. 11 through 16 (fig. 4). Springs that resulted from the downcutting increased the discharge of the sandstone and caused an adjustment of the hydraulic system. Near the outcrop area, the springs lowered water levels in the sandstone enough to cause a change from artesian to water-table conditions.

Meyboom (1960) calculated that the discharge from those springs today constitutes only a very small percentage of the flow of the Milk River. He also calculated that the river contributes only a very limited amount of recharge to the sandstone. The main intake area of the Milk River sandstone is at its surface exposure in the Sweet Grass Hills in Montana as evidenced by the steep hydraulic gradient shown on the potentiometric surface map (fig. 8).

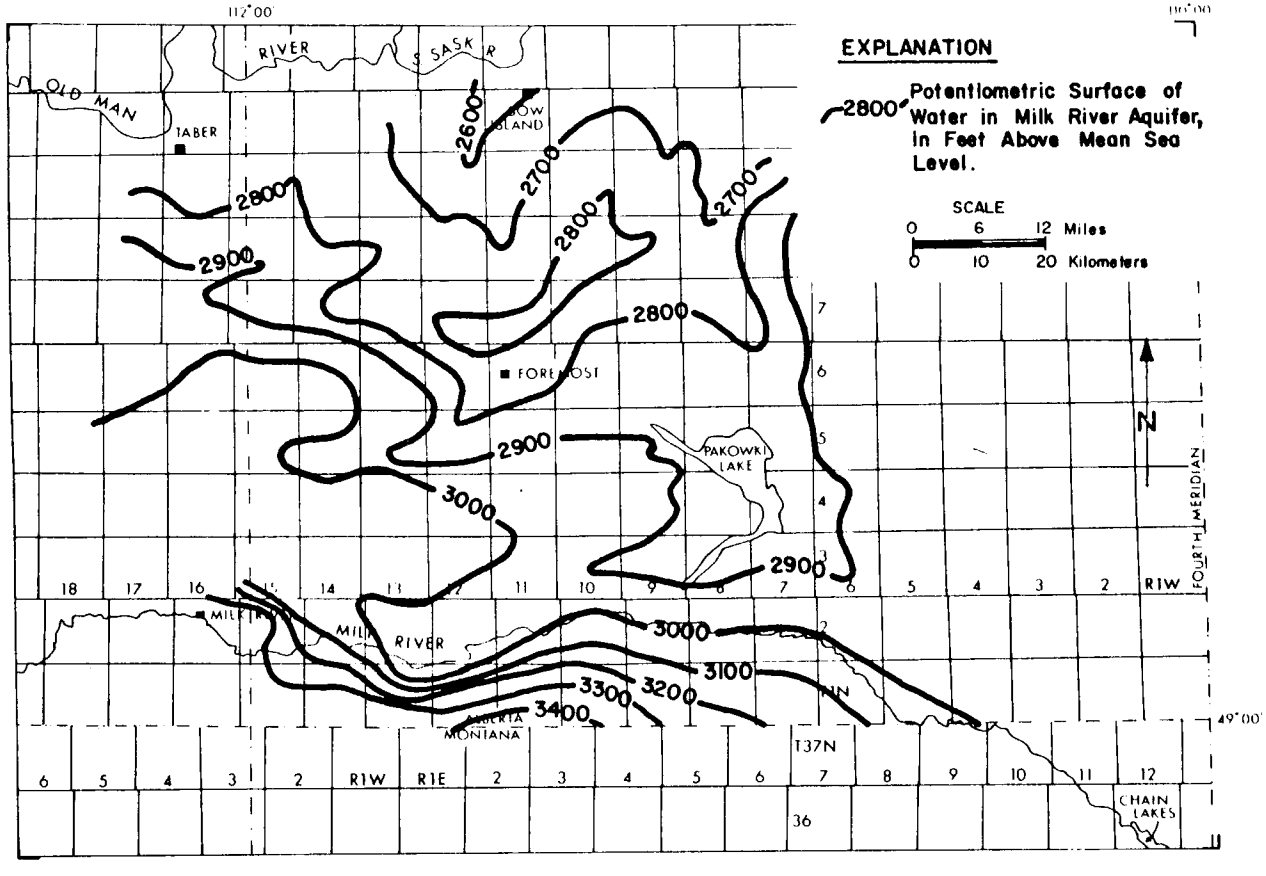

Figure 8. Potentiometric surface of the Milk River aquifer. -- After Meyboom (1960, fig. 16)

A large number of short field tests were conducted in the late 1950s to obtain transmissivity values for the Milk River sandstone. The tests involved capping flowing wells and recording the pressure response for 10 to 720 minutes. A map of the results from these tests (fig. 9) shows a northwest-trending zone of high transmissivity values, which closely coincides with a zone of thick sandstone deposits (fig. 10).

Meyboom (1960) estimated the storage coefficient for the Milk River sandstone by dividing the volume of water removed by the product of the head change and the surface area over which the head change was evident. His estimates were 3.0×10^{-4} and 3.5×10^{-4}.

The first continuous sandstone bed beneath the Milk River sandstone is the Bow Island sandstone. The hydraulic-head distribution of this formation, based on data from 161 drill-stem tests, was mapped by Schwartz and Muehlenbacks (1980) (fig. 11). Contours were generalized to delete areas where oil and gas production ongoing in the Bow Island sandstone has probably disrupted the natural hydraulic head in the aquifer. The figure shows the same general flow direction as are evident in the Milk River sandstone: generally from south to north.

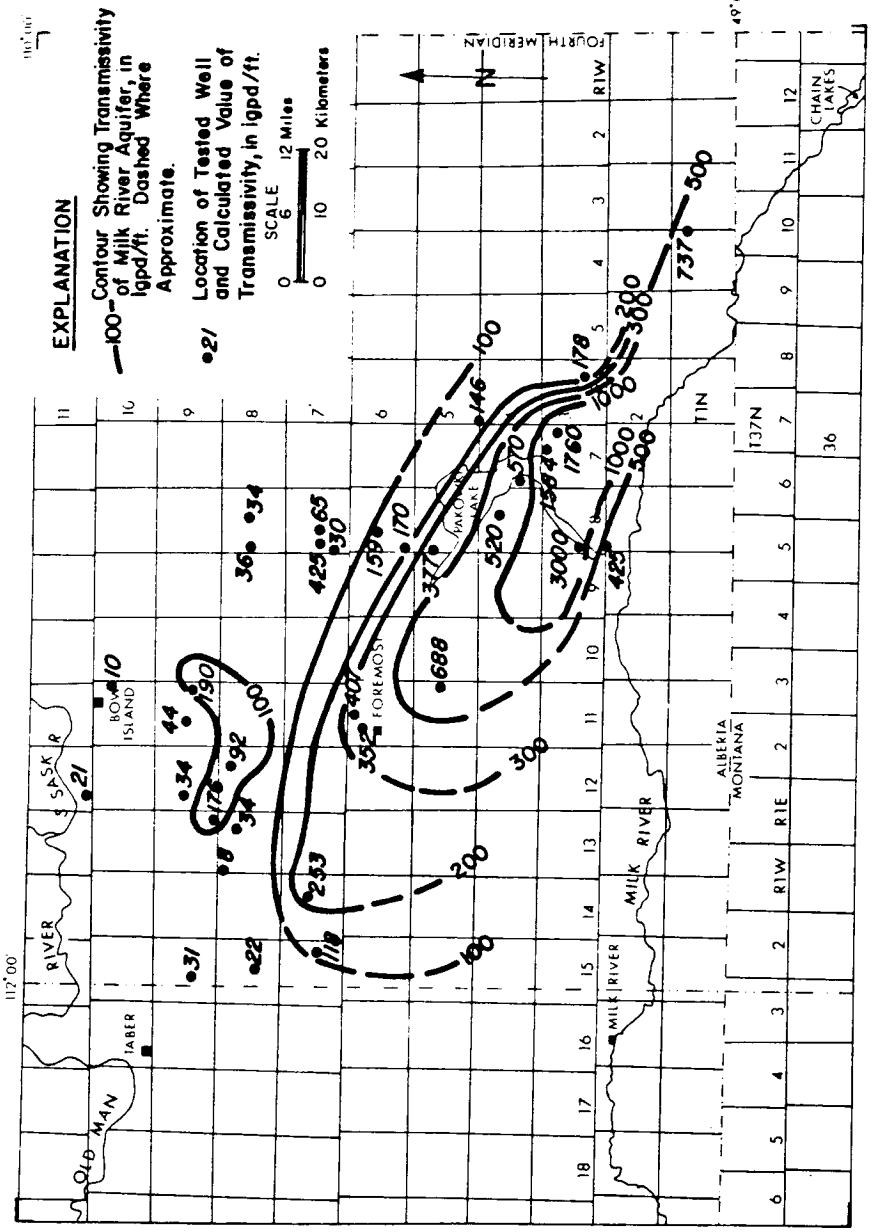

Figure 9. Areal variation of transmissivity of the Milk River aquifer

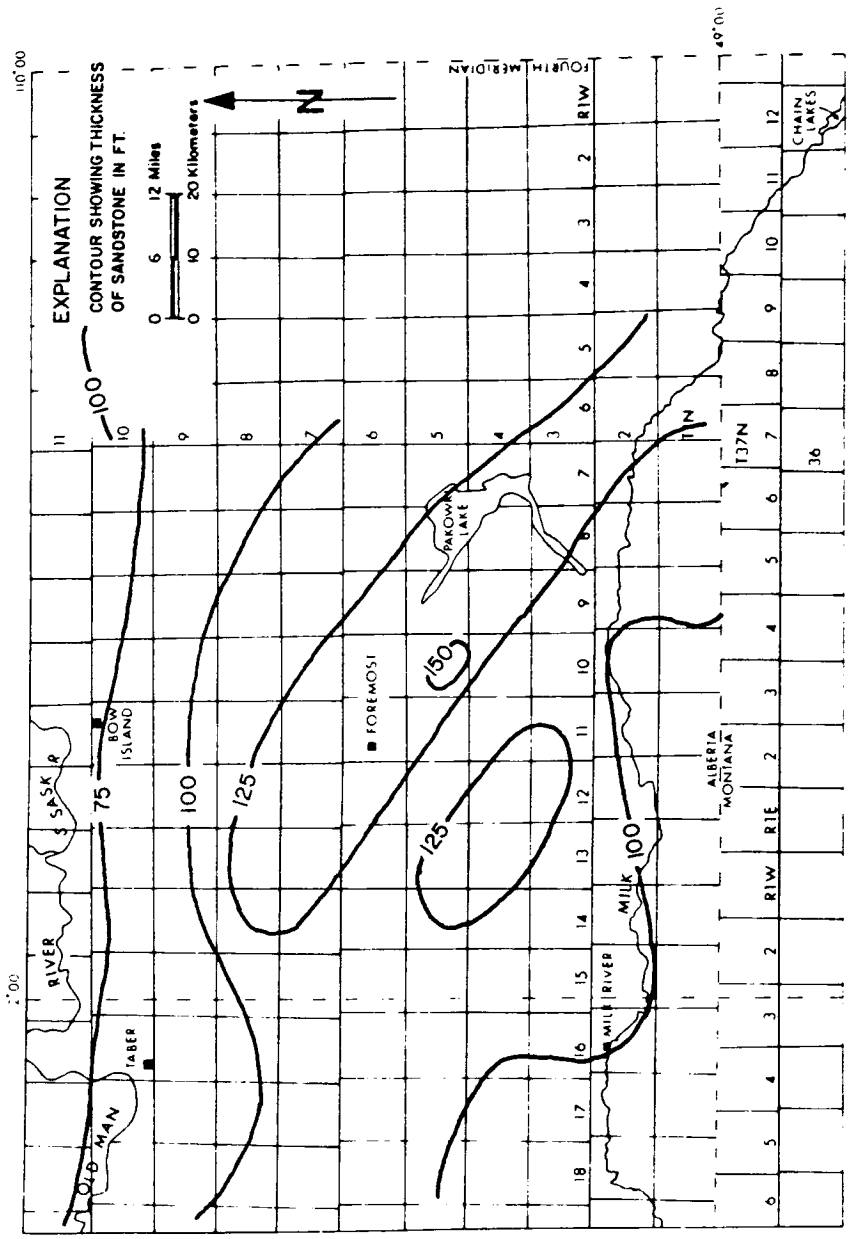

Figure 10. Isopach of sandstone in the Milk River aquifer

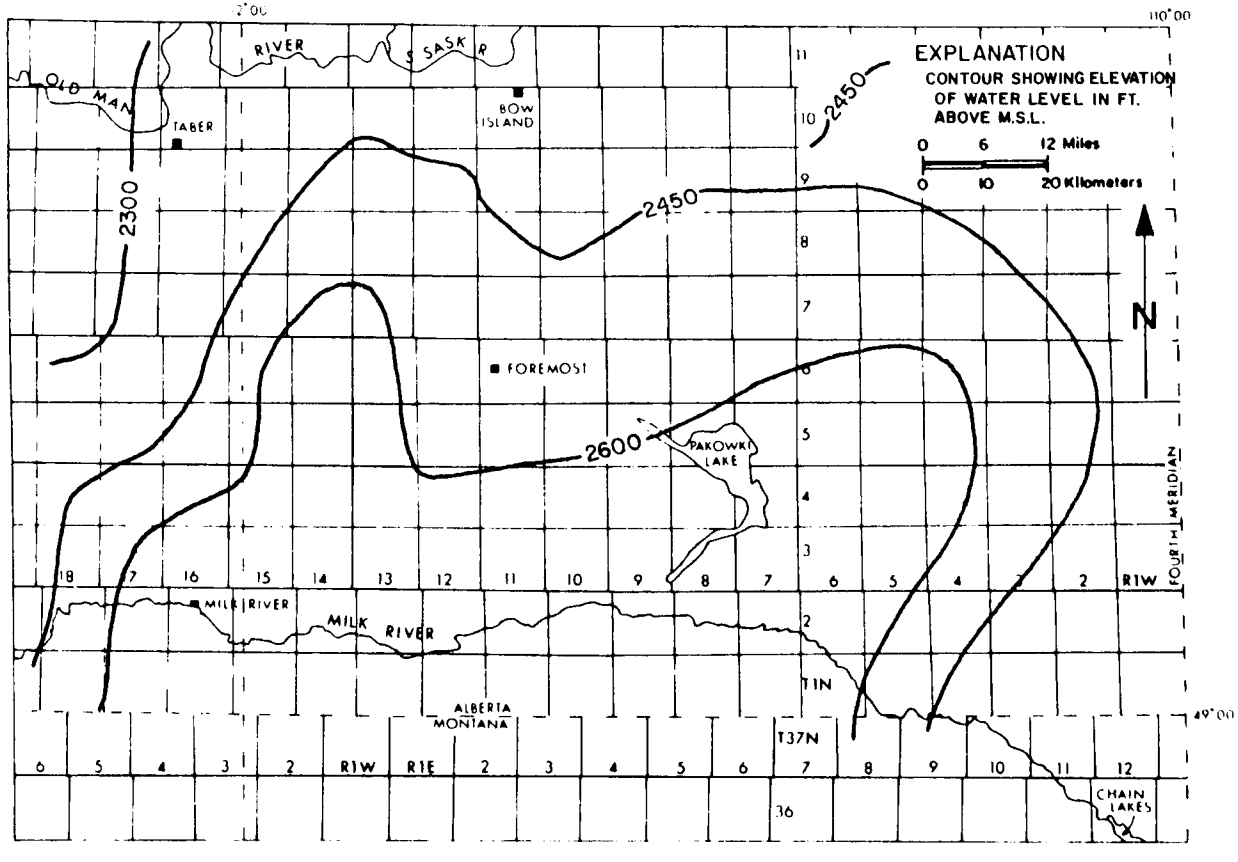

Figure 11. Potentiometric surface of water in the Bow Island sandstone. -- Generalized from Schwartz and Muehlenbachs (1980, fig. 2).

GROUND-WATER CHEMISTRY

The chemistry of the water from the Milk River aquifer has been previously described by Meyboom (1960), Borneuf (1976), and Schwartz and Muehlenbachs (1979). Hitchon and Freidman (1969) also described the formation's fluids from the western Canada sedimentary basin; however, only a few of their samples were from the Milk River sandstone.

Sampling Procedures

For the present study, samples were collected from 45 wells and two streams during the summers of 1979 and 1980. Five of the well-water samples were discarded after it was realized that the wells either had leaky casings or were screened in zones other than the Milk River sandstone. Locations of the sampled sites are shown on figure 12.

Field measurements were taken for carbonate and bicarbonate ion concentrations, pH, and temperature at each site. Chloride was precipitated as AgCl from sample water at all well sites for later analysis of chloride isotope concentrations, and carbon was precipitated as $BaCO_3$ at 12 wells for carbon isotope analysis. The procedures involved in separating the carbon and chloride are described in Appendix A. Dissolved oxygen in water from flowing wells was measured with a YSI-51A dissolved-oxygen meter (Yellow Springs Instruments). Because the results were neither reproducible nor consistent with expected concentrations based on observations of

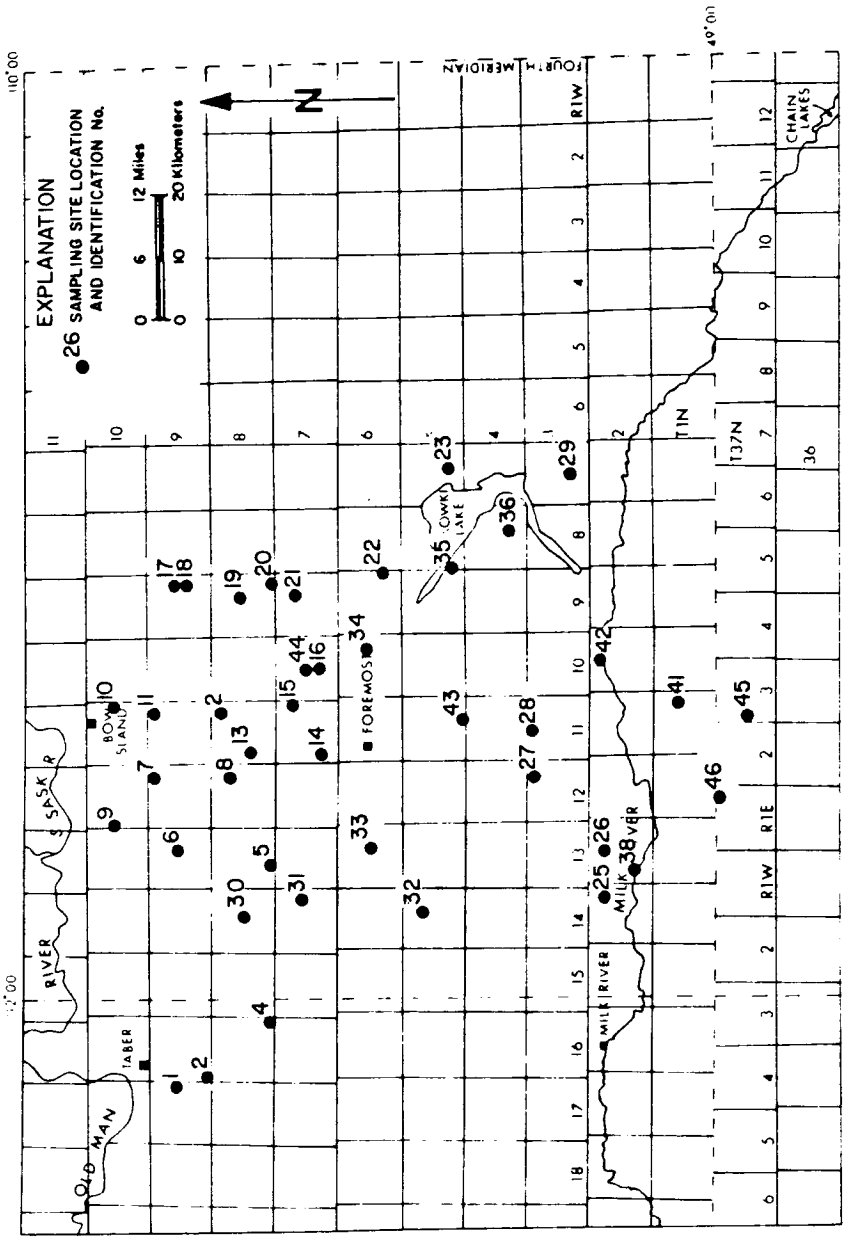

Figure 12. Sampling site locations for isotope and ion geochemistry

methane in the water, this information was disregarded in the geochemical interpretation. Field observations were made for hydrogen sulfide and methane in the water. Hydrogen sulfide could be smelled at several of the well sites. A Hach lead acetate hydrogen sulfide kit, made up of a small plastic jar, filter paper, and an Alka Seltzer tablet, was used to quantify the hydrogen sulfide concentration, but only site 32 had a concentration above the lower detection limit of 0.1 ppm. Many wells produce methane; this was noted but concentrations were not measured.

Half-liter samples of raw and HNO_3-treated water were collected at each site. The University Analytical Laboratory at The University of Arizona analyzed each for calcium, magnesium, sodium, potassium, total iron, sulfate, fluoride, chloride, and total dissolved solids. The University of Arizona Laboratory of Isotope Geochemistry analyzed samples for the nuclides deuterium, oxygen-18, carbon-13, and carbon-14. Chlorine-36 analyses were completed only recently (September 1981) and are discussed only briefly in this thesis. Appendix B lists the results of all analyses.

The areal distribution of the major cations and anions are shown in figures 13 through 19. These figures were developed from the data presented in Appendix B. In general, the sodium, chloride, and bicarbonate concentrations are lowest in the south and increase toward the north, whereas the total dissolved solids, calcium, and magnesium are most concentrated in the south and north and lowest in the central region of the study area. For all ions except sulfate, there is a noticeable southeast-northwest trend of low concentrations, which

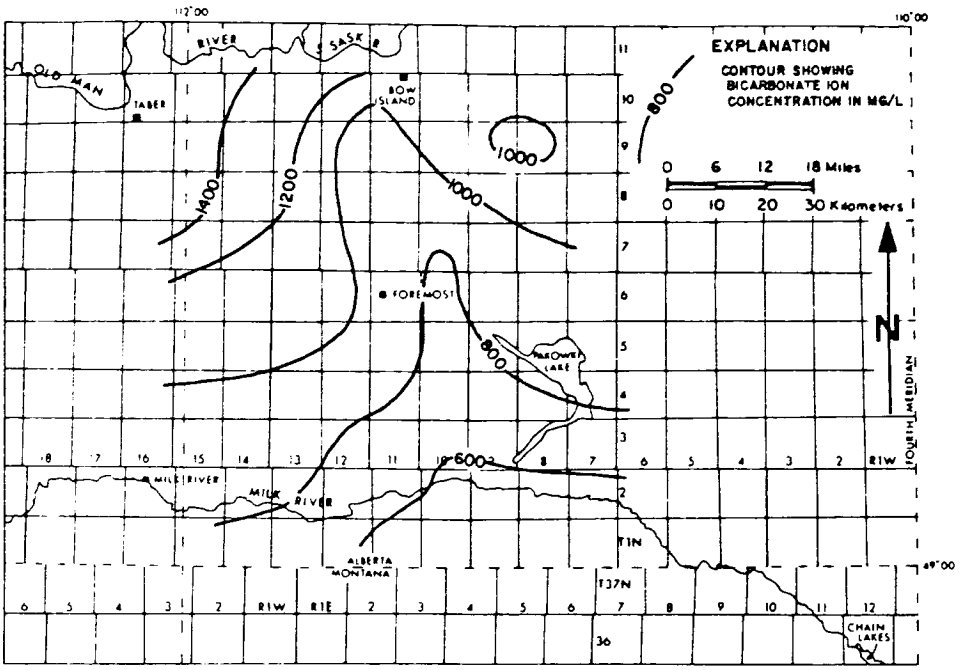

Figure 13. Areal variation of bicarbonate ion concentration in the Milk River aquifer

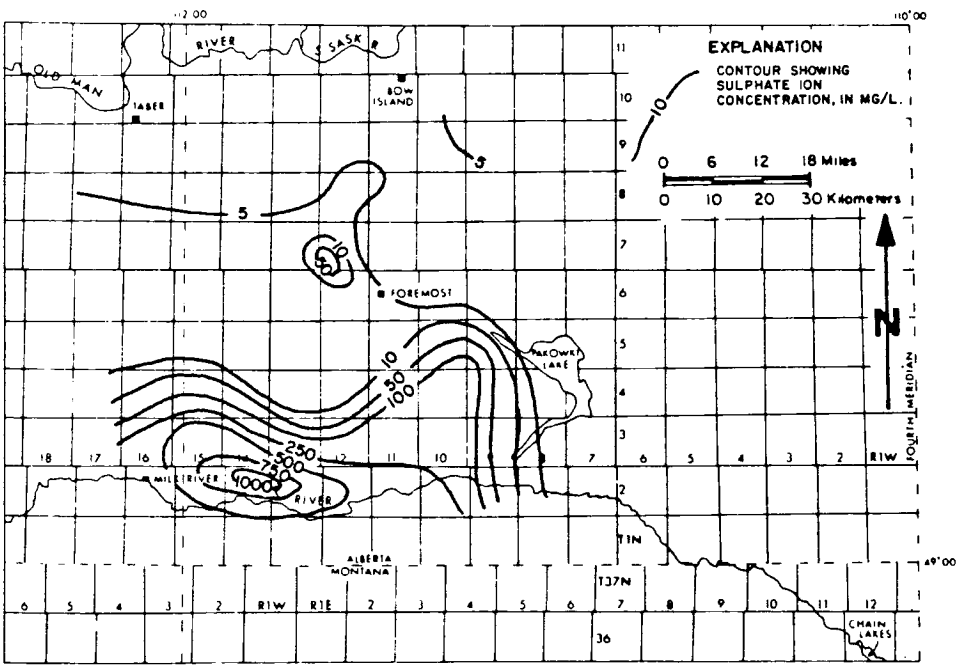

Figure 14. Areal variation of sulfate ion concentration in the Milk River aquifer

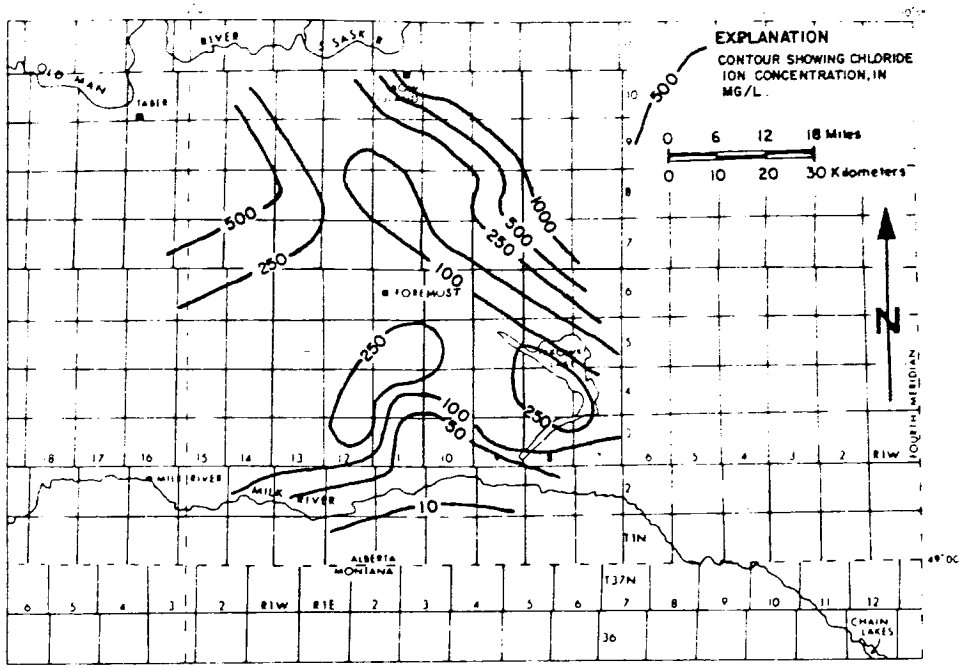

Figure 15. Areal variation of chloride ion in the Milk River aquifer

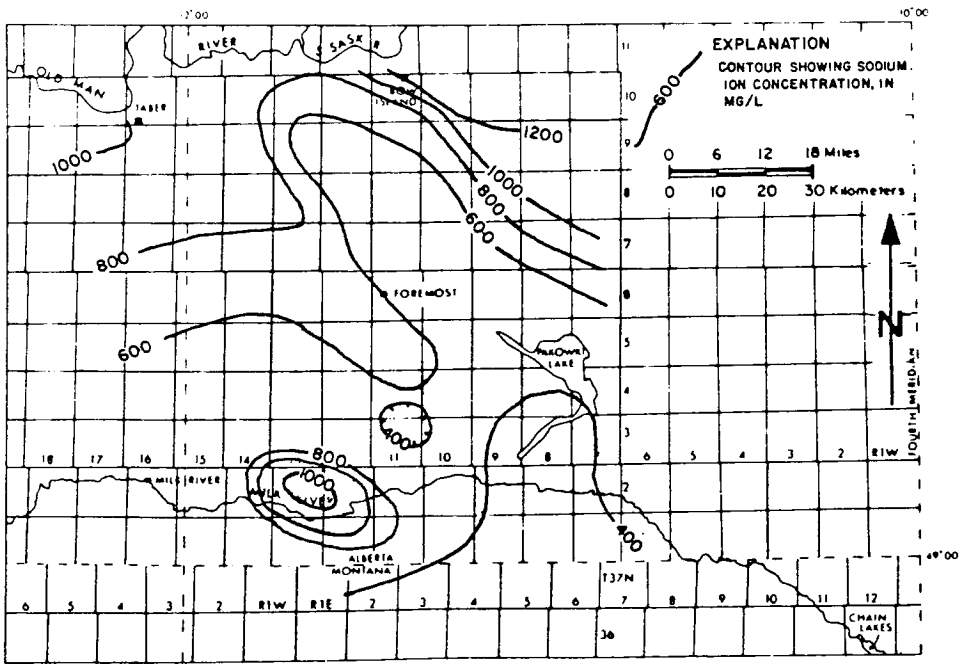

Figure 16. Areal variation of sodium ion in the Milk River aquifer

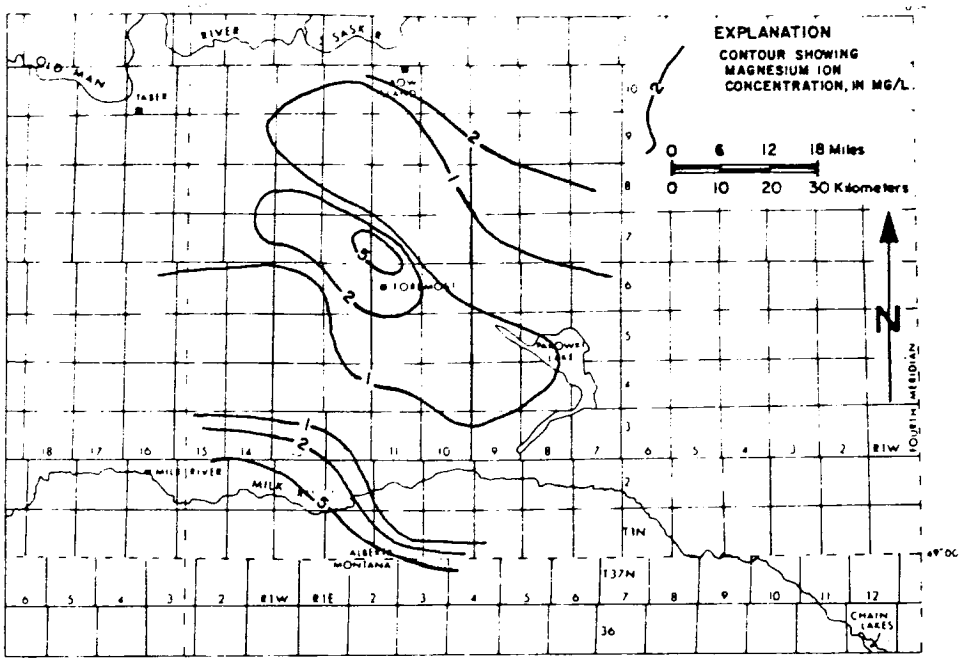

Figure 17. Areal variation of magnesium ion in the Milk River aquifer

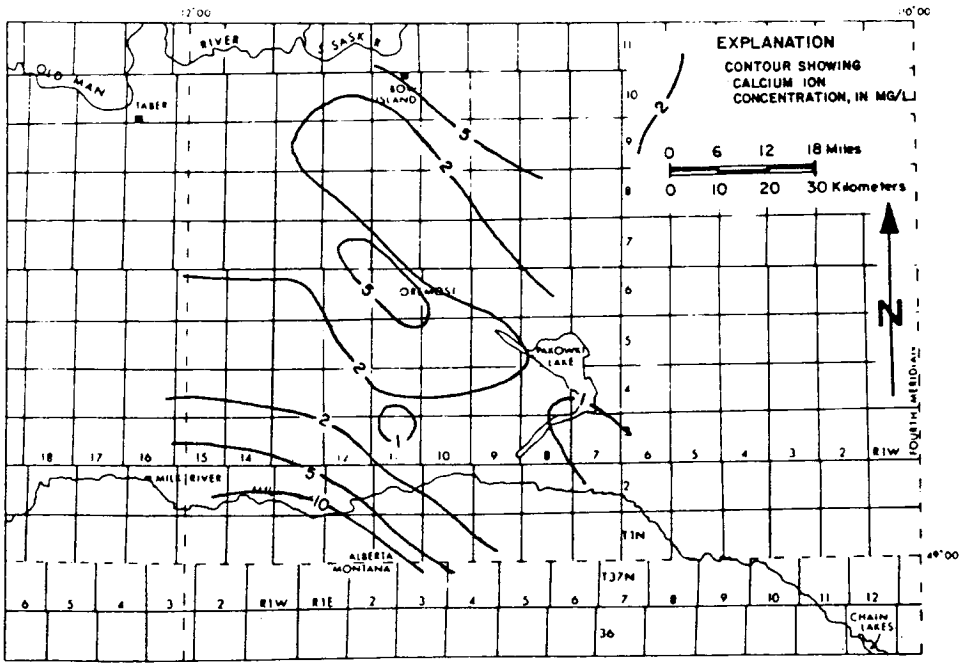

Figure 18. Areal variation of calcium ion in the Milk River aquifer

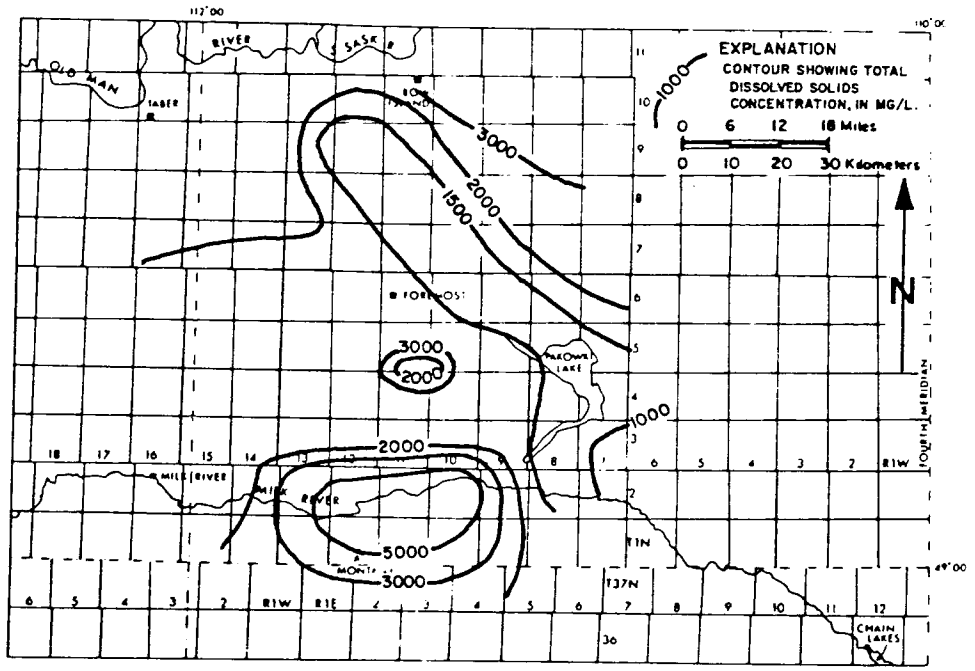

Figure 19. Areal variation of total dissolved solids concentrations in the Milk River aquifer

closely corresponds to the area of high transmissivity. Also noticeable is an area of high concentration of sodium, sulfate, and total dissolved solids in the southwestern part of the study area along the Milk River. In this area, the sandstone is fairly shallow and is commonly exposed at land surface along stream channels. Sulfate concentrations are greatest in the south and decline toward the north.

Results of analyses for oxygen-18 and deuterium are shown in Table B-2 (Appendix B). Figures 19 and 20 show the areal distribution of δD and $\delta^{18}O$ (per mille relative to standard mean ocean water, SMOW). These figures depict δD and $\delta^{18}O$ values of about $-155°/_{oo}$ and $-20°/_{oo}$, respectively, in the southern study area increasing to about $-65°/_{oo}$ and $-9°/_{oo}$ toward the north. All of the above figures are similar to those developed by Schwartz and Muehlenbachs (1979) based on their sampling from the same aquifer.

Samples from 12 wells were analyzed for $\delta^{13}C$ ($°/_{oo}$ relative to Peedee Belemnite, PDB) and ^{14}C (% modern). The results of these analyses are shown in Appendix B and in figure 22. The ^{14}C values are greatest in the south and decrease toward the north. The $\delta^{13}C$ values are smallest in the south-central area (approximately $-13°/_{oo}$ to $-12°/_{oo}$) and, although greater toward the north, do not follow a noticeable trend in the north.

The patterns of isotope and ion concentrations indicate that a variety of physical, chemical, and biological processes may be operating in the system. The deuterium and oxygen-18 composition of the formation waters suggest a variety of mechanisms for the causes of the changes seen. In the following sections, several possible processes

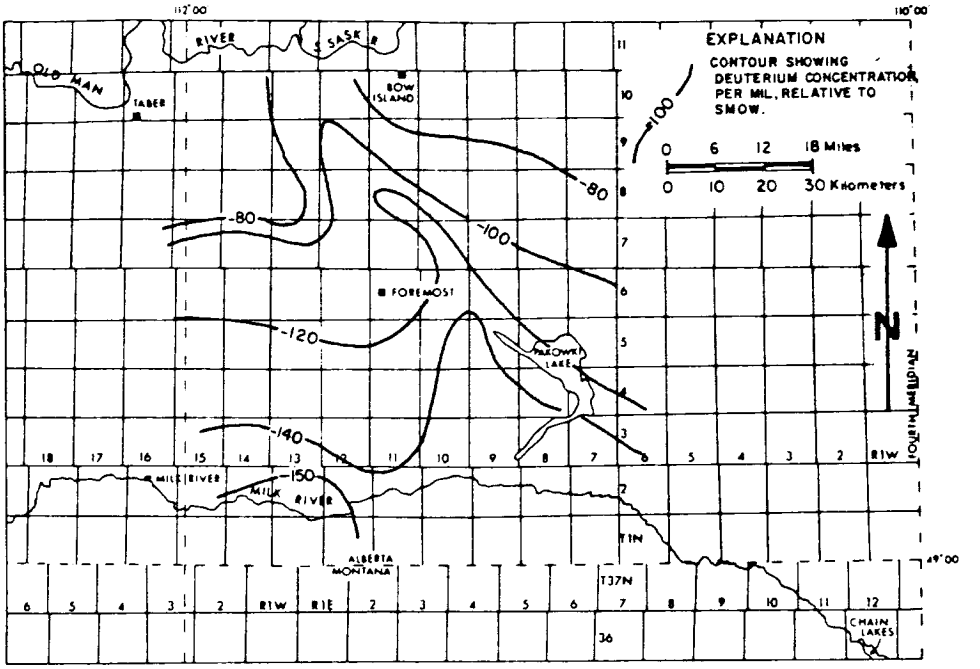

Figure 20. Areal variation of δD in the Milk River aquifer

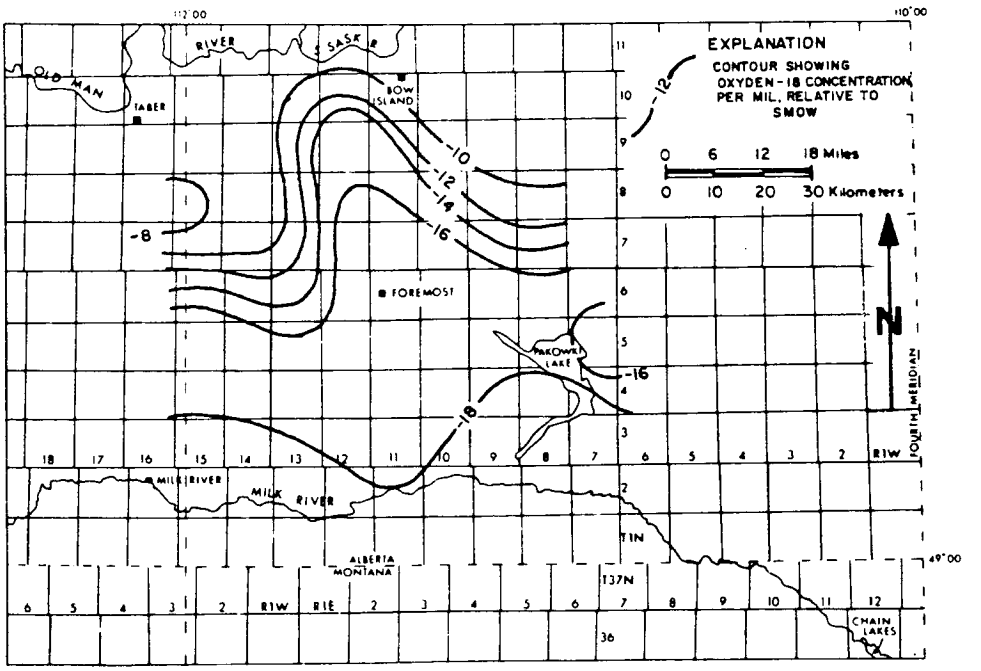

Figure 21. Areal variation of $\delta^{18}O$ in the Milk River aquifer

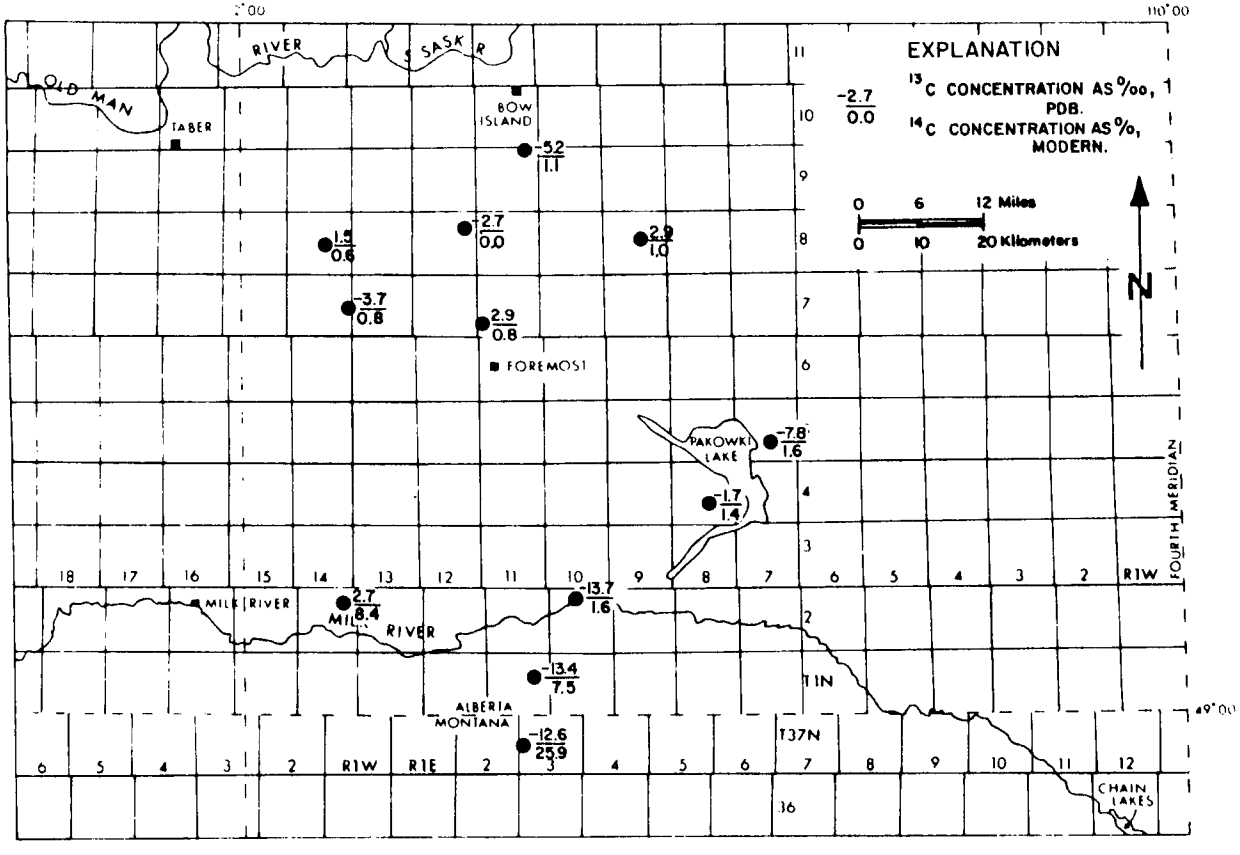

Figure 22. Sample site locations and carbon isotope concentrations in the Milk River aquifer

that can explain the changing isotopic composition of the formation water will be presented and discussed on the merits of the isotope and ion geochemistry.

Hydrogen and Oxygen Isotopes

The $\delta^{18}O$ values are plotted against the δD values in figure 23. Isotopically lightest waters (represented by the most negative values of concentration) fall very near the meteoric line and are unaltered surface and near-surface waters from sampling sites in the southern, or recharge, portion of the study area. The progression of data points, from isotopically lightest to heaviest, follow a sampling path from the recharge area in the south toward the north. The data points tend to fall below the meteoric line away from the recharge area. A line of best fit through these data points (as calculated by linear regression) has a slope of 7.5, as compared to the slope of 8.0 for the meteoric line. The possible mechanisms for the changing isotopic composition of ground water in the Alberta Basin have been discussed by Clayton and others (1965), Graf and others (1965), Hitchon and Friedman (1969), and Schwartz and Muehlenbachs (1979, 1980). Those mechanisms that could cause the noted changes are: (1) climatic change over time causing changes in the isotopic composition of precipitation and, thereby, recharge; (2) isotopic exchange between water and minerals or between water and hydrogen compounds such as hydrocarbons and hydrogen sulfide in the water; (3) isotopic effects caused by filtration through membranes; and (4) mixing of meteoric with connate waters. The isotopic variation observed may also be caused by a combination of any of

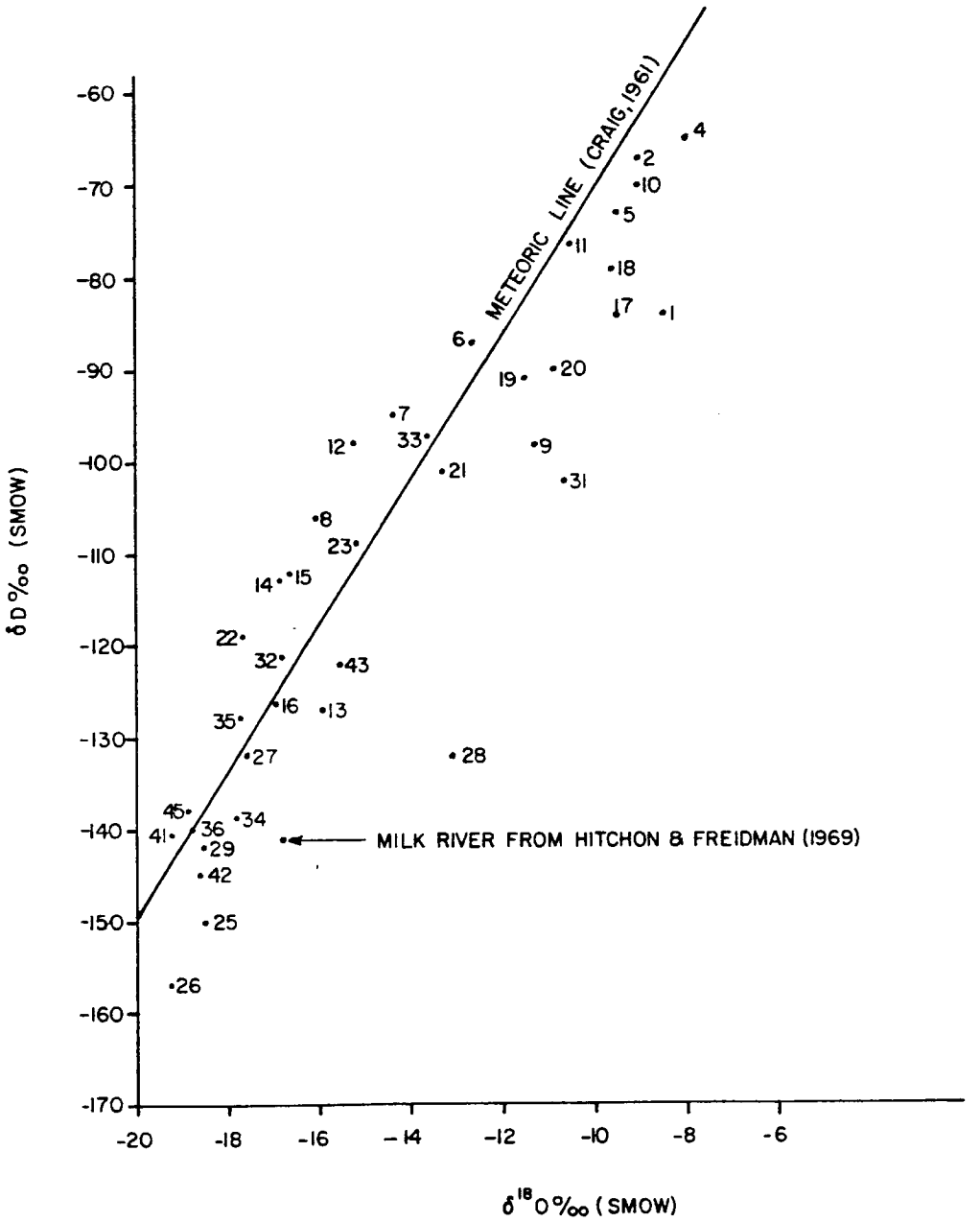

Figure 23. Plot of δD vs. $\delta^{18}O$ for samples from the Milk River aquifer

the aforementioned mechanisms. Following is a discussion of each of the hypotheses mentioned above.

Climatic Change

The proposed model of climatic change would require that the water entering the aquifer in the past was enriched in oxygen-18 and deuterium by about $11°/_{oo}$ and $90°/_{oo}$ with respect to present meteoric waters. According to Dansgaard (1964), an increase in temperature of 4°C would be accompanied by an increase of δD of $22°/_{oo}$. Therefore, recharge water with the concentrations of isotopes of the oldest waters would indicate that the climate was about 16°C warmer than the present one. The data pattern shown in figure 23 could be accomplished by a continued cooling of the climate accompanied by oxygen exchange between the wall rock and the water. The latter hypothesis would explain the shift of the data below the meteoric line.

The hypothesis of continued cooling of the climate is contradicted by a great deal of paleoclimate data from pollen and core studies, including an core study by Van Donk (1976), which included the past 2.3 million years. Van Donk used ^{18}O in a well-dated equatorial Atlantic core to indicate paleoclimates. He found that in the past 500,000 years there have been four prominent interglacial periods, including the present one, and three prominent glacial periods. The glacial-interglacial periods would indicate a cyclic warming and cooling of the climate rather than continued gradual cooling. Also, Heusser (1977) determined that temperatures, rather than having continued to cool over the years, were about 7°C to 9°C cooler during the Wisconsin

glacial advance. This evidence would lead to rejection of the changing-climate hypothesis.

Isotopic Exchange

Concurrent exchange of oxygen between the water and wall rock and of hydrogen between water and minerals or hydrogen compounds could cause the observed trends in isotopic composition seen in the Milk River aquifer. In their studies of the origin of saline formation waters in four basins, including the Alberta Basin, Clayton and others (1965) found that extensive oxygen exchange had taken place between the water and the wall rocks. The geochemical and isotope data they used were from samples of oil-field brines taken from various depths throughout the basin. Their conclusions were based on the excellent agreement between data plots of $\delta^{18}O$ versus the well temperature and the equilibrium curves for the calcite in the wall rocks. Calcite $\delta^{18}O$ ($+22.3°/_{oo}$ for the Alberta Basin) for each basin was chosen to give the best fit for the data. The brine samples used in the Alberta Basin study, however, had a temperature range of about 25°C to 100°C, whereas temperatures in the Milk River aquifer ranged from about 8°C to 18°C, and it is as yet questionable whether carbonate equilibrium will be reached in waters with temperatures of less than 50°C. Clayton and others questioned whether equilibrium with carbonates can be reached in aquifers such as a sandstone aquifer with carbonate-poor rocks. Hitchon and Friedman (1969), in their study of the formation waters of the Alberta Basin, performed a multiple regression analysis on oxygen isotope data from waters from sandstone and

limestone aquifers and found that oxygen-18 exchange is effective in both types of reservoirs because sufficient carbonate was present as either cement or host rock in all systems to allow equilibrium.

Figure 24 shows the plot of $\delta^{18}O$ versus well temperature for the samples collected during this study. The equilibrium curve for calcite ($\delta^{18}O = 22.3°/_{oo}$) is also shown on this figure. The ^{18}O-enriched water approaches the equilibrium curve, possibly indicating that the oxygen shift is due to equilibrium with host rocks. If equilibrium is the controlling mechanism for the ^{18}O content of the water, it is unclear whether equilibrium was reached in response to the temperature reaching a certain level (approximately 13°C according to the figure) or because the reaction at the residence temperatures is very slow.

Isotopic exchange between water and hydrogen-containing compounds such as hydrocarbons can cause a deuterium enrichment in the waters in which they are formed. Deuterium exchange between H_2S and H_2O is used commercially in the production of heavy water and will take place in nature where H_2S occurs. Although small amounts of H_2S have been detected in the Milk River aquifer, the reservoir of hydrogens in the water is so large relative to the reservoir of hydrogen in H_2S that the shift of deuterium concentration in the water would be insignificant.

Wells in the Milk River aquifer commonly produce methane. During sampling in the summer of 1980, I noted many wells producing methane gas with the water (fig. 25). Although no measurements of the gas volume were made, the gas concentrations were estimated to have ranged from only a few percent to as much as about 50 percent of

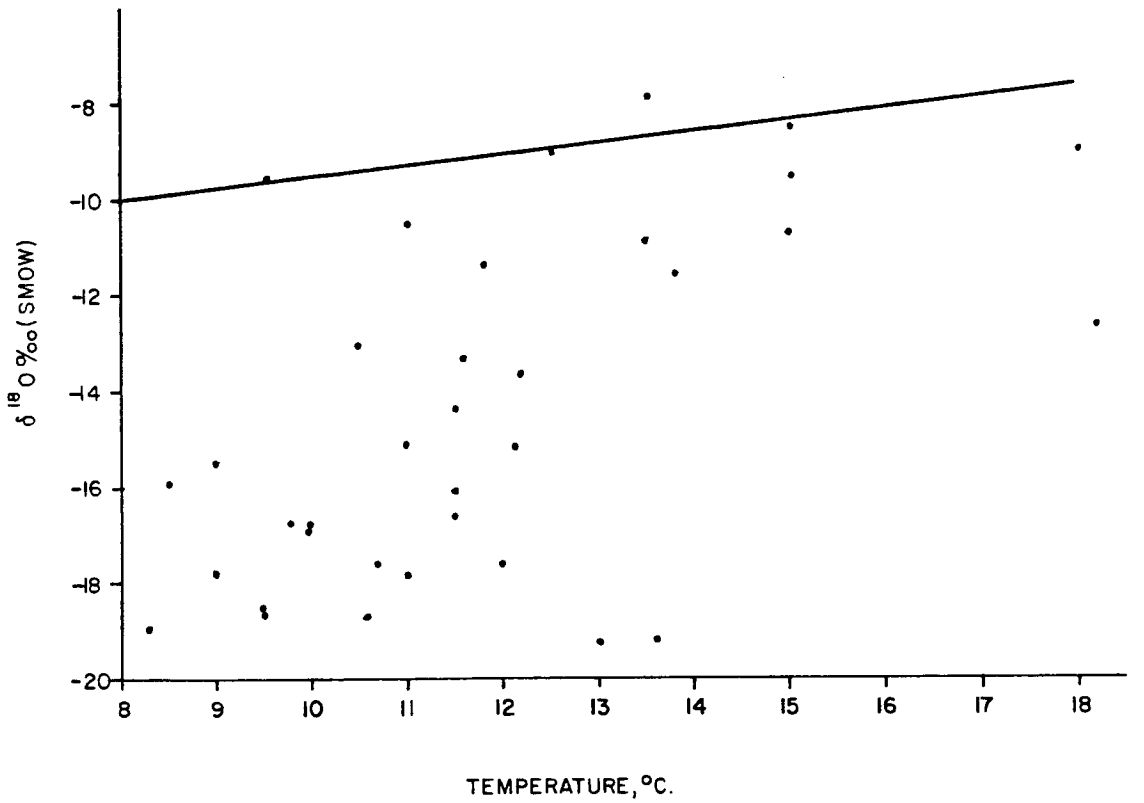

Figure 24. Plot of $\delta^{18}O$ vs. water temperature in the Milk River aquifer

Curve shows theoretical equilibrium of water and rock (using $\delta^{18}O_{calcite} = 22.3°/_{oo}$, after Clayton et al., 1965).

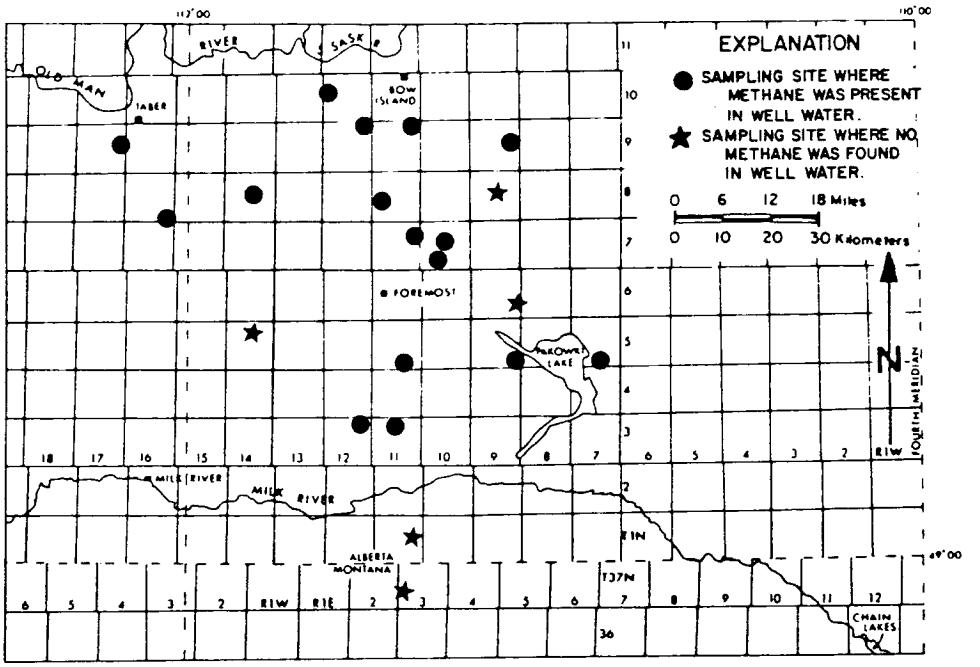

Figure 25. Locations where presence or absence of methane in Milk River aquifer was noted during field sampling August 1980

the volume expelled from the wells. The average methane production was probably between 10 and 20 percent by volume. Schoell (1980) found that biogenic methanes were depleted of deuterium by approximately 160°/$_{oo}$ compared to the deuterium concentration of their associated waters and that the relationship between deuterium contents of the two suggested that all of the hydrogen in the biogenic methanes is derived from their associated waters.

Assuming that the δD of the gas in 160°/$_{oo}$ lighter than the δD of the surrounding water in the Milk River aquifer, mass balance calculations indicate that a 90°/$_{oo}$ shift in the deuterium content of the formation water would require 31.5 liters of gas to be produced per liter of water (at 25°C and 1 atmosphere). If the more likely value of 10% methane by volume were used in the calculation, there would be only an enrichment of about 0.3°/$_{oo}$ of deuterium in the water.

There remains a possibility of isotopic exchange between the formation water and sedimentary minerals, primarily clays, causing enrichment in deuterium. The extent of isotopic exchange between clay minerals in the temperature range of 100°C to 350°C has been measured for runs of up to 2 years (Hoefs, 1980, p. 145). A measurable hydrogen isotope exchange was observed at even 100°C. It is probable that all of the hydrogen isotope exchange occurred very early in the history of the clays and that there is no isotopic effect. In any case, the reservoir of hydrogen molecules in the water dominates the number of hydrogen molecules found in the mineral structure of the clays and the change in deuterium concentration in the water due to the deuterium exchange would be small.

The hypothesis that the shifts in oxygen-18 and deuterium are due to concurrent wall-rock exchange of oxygen and mineral and hydrogen compound exchange of hydrogen is therefore rejected. Although some of the water is in isotopic equilibrium with the wall rock, most of the water is not, indicating that wall-rock exchange may not be occurring over much of the aquifer. And, based on mass balance equations, exchange of hydrogens in water with minerals and hydrogen compounds would produce only a small shift in the deuterium concentration compared to the large shift observed.

Filtration through Membranes

In the past two decades compacted clays and shales have been demonstrated to act as membranes that will allow solutes to pass through them in differing proportions. If a pressure gradient is applied across the membrane, fluid in the formation will move through the membrane but some of the solutes will be retained on the side of the membrane with the greater hydrostatic head. This phenomenon is referred to as ion filtration. The fractionation of oxygen and hydrogen isotopes in the water accompanies ion filtration during passage through membranes.

Ion filtration accompanied by isotopic fractionation has been suggested as an explanation of the origin of formation waters in the Illinois, Michigan, and Alberta basins and the Gulf Coast by Graf and others (1965). Coplen and Hanshaw (1973) measured the isotopic fractionation effect in laboratory experiments using compacted montmorillonite discs. Kharaka and Berry (1974) attributed the isotopic

and ionic variation of waters in the Kettleman North Oil Field in California in part to membrane effects. Schwartz and Muehlenbachs (1979) suggested that these mechanisms might control the ionic and isotopic variations of the waters in the Milk River aquifer.

After using a complex normalization procedure on the isotope concentrations of the formation, Graf and others (1965) found that the differences in the deuterium and ^{18}O concentrations from the input to the residual side of the membrane ($\Delta\delta D$ and $\Delta\delta^{18}O$) were $40°/_{oo}$ and $12°/_{oo}$, respectively. Kharaka and Berry (1974) found a residual $\Delta\delta D$ of $45°/_{oo}$ and $\Delta\delta^{18}O$ of $14°/_{oo}$ at Kettleman North Dome. When Coplen and Hanshaw (1973) forced a weak aqueous NaCl solution under a 100-bar gradient through a clay disc compacted by 330 bars, the experiment yielded a $\Delta\delta D$ of $2.5°/_{oo}$ and $\Delta\delta^{18}O$ of $0.8°/_{oo}$ in the residual solution. In each of the examples, the ratio of $\Delta\delta D$ to $\Delta\delta^{18}O$ was about 3. Linear regression analysis on the isotopic concentrations of samples from the Milk River aquifer yielded an average slope of about 7.5; the ratio is greatest for data near the recharge zone and is smaller for samples from the north.

Although isotopic fractionation during membrane filtration has been demonstrated, the mechanism by which it occurs is not clearly understood. Several explanations have been suggested. One possible explanation of the fractionation could be molecular diffusion. Because the H_2O, $H_2{}^{18}O$, and the HDO each have different masses, they would be expected to diffuse at different rates. When momentum transfer is considered, the $\Delta\delta D$–$\Delta\delta^{18}O$ ratio would be expected to be 0.5. In each of the aforementioned cases, the ratio was much greater than 0.5

indicating that molecular diffusion is not the dominant mechanism involved in fractionation by membrane filtration.

Coplen and Hanshaw (1973) suggested a mechanism that involves hydrogen bonding to the clay particles. They proposed that the bonding is related to the mass of the atoms involved as opposed to the mass of the water molecule and that water molecules pass through the clay membranes by jumping from one adsorption site to another. Fractionation would occur because of the different bonding rates for each of the isotopic species. Phillips (1980) argued against such a mechanism's being the dominant cause of the observed fractionation. He argued that such a mechanism could cause a transient fractionation but not a steady-state difference between the inflow and outflow concentrations across a membrane. He further argued that differences in bonding rates would imply fractionation of soil water tightly bound to clay surfaces and cited experiments by several other investigators that would not support that.

A third mechanism, salt filtering, was discussed by Coplen and Hanshaw (1973) and Phillips (1980). The term "salt filtering" is used to indicate a mechanism by which the heavier isotopes of hydrogen and oxygen are somehow preferentially fractionated into a close, tightly bound sphere around ions in the water, which is then filtered through the clay membrane. Rejection of an ion by a membrane would be accompanied by rejection of all associated tightly bound water molecules. Coplen and Hanshaw (1973) rejected this hypothesis because they found the same amount of fractionation across a compacted clay membrane with both distilled water and 0.01 M NaCl water. Because both experiments

yielded the same results, they decided that salt filtering was not significant in the fractionation process.

Phillips (1980) arrived at the same conclusion for different reasons. He used a structure forming–breaking model of ion-water interaction and support from experiments of many other scientists to determine that ^{18}O is preferentially retained by most ionic solutions, whereas deuterium is preferentially retained by none. He argued that, if salt filtration were the cause of enrichment of deuterium and ^{18}O in the residual solution, both isotopes would have to be preferentially retained by the ions in solution and therefore salt filtration is probably not of major importance in producing the observed fractionation phenomenon.

Phillips hypothesized another mechanism for the fractionation of isotopes across clay membranes that is as yet unsubstantiated by laboratory experiments. He used a model to describe ions surrounded by a sphere of highly coordinated water molecules arranged radially around the ion surrounded by a second sphere of chaotic disorganized water molecules. Surrounding these two spheres is the bulk of water molecules, which is highly structured due to hydrogen bonding. The tendency of an ion to be a structure former or structure breaker depends on the size and charge of the ion. The smaller and more positively charged the ion, the greater its structure-forming ability, and the larger and more negatively charged the ion, the greater its tendency to be a structure breaker. Using theoretical arguments and observations from laboratory experiments to support his hypothesis, Phillips described the relative tendencies of water molecules containing

deuterium and ^{18}O to move into or out of the two spheres surrounding ions. He hypothesized that water molecules containing deuterium would be discriminated against in both spheres. Water molecules containing ^{18}O would be preferentially included in the inner sphere and they would be discriminated against in the outer sphere, but to a lesser extent than the deuterium-containing molecules. Phillips (1980) observed that clay membranes maintain pore solutions of high ionic strength in the presence of dilute external solutions. The water molecules entering the clay membrane would constantly pass in and out of the structure-broken (outer) sphere around an ion but would not be significantly affected by the tightly bound inner sphere. He hypothesized that, because the structure-broken spheres preferentially exclude molecules with deuterium and ^{18}O, there would be a back diffusion of molecules containing these isotopes and therefore a fractionation of the isotopes across the membrane. Because deuterium is excluded from the structure-broken regions around ions to a greater degree than ^{18}O, it would be expected that $\Delta\delta D/\Delta\delta^{18}O$ would be greater than 1. Phillips then used a Rayleigh distillation-type equation to mathematically model the system.

Graf and others (1965) found the slope of their normalized isotope data to be 3 ($= \Delta\delta D/\Delta\delta^{18}O$). They argued that this slope should be a maximum because part of the observed ^{18}O effect probably resulted from equilibration with host rocks. They considered a slope of 0.5 to be a minimum because that would be the slope if diffusion were the dominant mechanism. It seems to me that a slope of 3 for their data is not a maximum, but rather a minimum. Most of their samples

were taken from oil-field brines at temperatures between 15°C and 100°C. Many of these samples had already reached equilibrium with the host rocks (Clayton and other, 1965). The effect of equilibration would be to shift the $\delta^{18}O$ toward zero, thereby increasing $\delta^{18}O$ and decreasing the slope of the δD-vs.-$\delta^{18}O$ line.

Coplen and Hanshaw (1973) found a slope of 3.1. They stated that, based on an adsorption dominant mechanism for fractionation, the relative isotopic fractionation would depend on many factors that include temperature, composition of adsorbant, and the type of bonding involved.

Phillips (1980) argued that the slope should be positive but that a slope of 3 is not required. He also suggested that the variation in the slope for the data from the Milk River aquifer may be due to the ionic concentration of the pore fluid in the clay membrane.

Past experiments have shown that the minimum differential pressure under which clays will act as ultrafilters is between 200 and 500 psi (Graf and others, 1965). In experiments on concentrations changes of pore solutions during clay compaction, Englehardt and Gaida (1963) found that the compaction of clays was essentially irreversible when the load was removed. They explained this phenomenon in terms of aggregate destruction by compression. Their findings indicate that, if clays overlying or underlying the Milk River aquifer ever experienced a load of 200 to 500 psi, the clays would remain acting as ultrafilters because the clay would not rebound. Flint (1971) stated that the Canadian plains in southern Alberta had 300 to 700 m of ice during the Late Wisconsin glacial stage and as much as 900 m during the Early

Wisconsin. If the 200 to 500 psi criterion were used, only 140 to 350 m of ice would be required to compress the clays enough for them to act as ultrafilters. These facts support the hypothesis of membrane filtration.

Mixing Phenomena

The trend of the hydrogen and oxygen isotope data suggests that some type of mixing phenomenon may be responsible for the chemical nature of the water. In a simple mixing model with two fluids of differing ionic and isotopic composition, a graph of δD vs. $\delta^{18}O$ would show a straight two-component mixing line between the two fluids.

Hitchon and Friedman (1969) suggested that the waters in the western Canada sedimentary basin may have originated by mixing meteoric water with modified marine or nonmarine water present in the rocks combined with extensive exchange of oxygen isotopes between the water and host rocks. The mixing of meteoric water with connate water in the rock would imply that the hydrogen and oxygen isotopes would plot as a straight line from the present-day meteoric water to SMOW. In such a model, if it is assumed that the deuterium in the waters were essentially unaltered in time, the deuterium concentration present deep in the Milk River aquifer suggests that the connate waters have been at least partially displaced by the fresher water. The data plot falls below a straight mixing line, which would be explained by oxygen exchange with host rocks.

One argument against such a model was raised by Schwartz and Muehlenbachs (1979). The deuterium values of $-80°/_{oo}$ to $-90°/_{oo}$ in

the deepest formation waters would indicate a mixture of approximately 60% meteoric water and 40% connate water (assuming the connate water had the isotopic composition of sea water), whereas the chloride concentration of 1400 mg/L suggests that less than 10% of the water can be connate.

Although mixing of meteoric and connate waters does not seem to be a probable mechanism, it is possible that the deeper Milk River aquifer water is representative of some nonmarine water that evolved sometime during the geologic history of the formation.

A third mixing mechanism, megascopic dispersion, has been proposed by Schwartz and Muehlenbachs (1979). Megascopic dispersion is dispersion caused by large formational heterogeneities such as regional stratigraphy that are responsible for changes in the direction and velocity of fluid flow. For their model, they visualized the aquifer as part of a large regional system as opposed to an isolated hydrologic unit isolated by confining layers. They suggested that the isotopic patterns may reflect the cumulative effect of adding more saline, isotopically heavier water from the shale unit immediately below to the Milk River aquifer. They have found isotopic and ionic patterns in the Bow Island sandstone, the next continuous sandstone below the Milk River, to be similar to those observed in the deepest portion of the Milk River aquifer. Schartz and Muehlenbachs recognized the present apparent downward head gradient in the formations beneath the Milk River, but they argued that the present-day flow pattern may not be the one responsible for the observed chemical patterns.

Although such a scenario is possible, compelling evidence to suggest that the direction of head gradient from the Nilk River aquifer to the Bow Island sandstone has changed in many millions of years is lacking. In the present system, a 300-foot downward head gradient exists across the shales that separate the Milk River aquifer from the Bow Island sandstone.

In summary, the oxygen and hydrogen isotope patterns in the Milk River aquifer would indicate that either or both membrane filtration and dispersive mixing may be responsible for the composition of the ground water. The proposed mechanisms involved in membrane filtration are hypothetical, and there is controversy about what relative isotopic changes should occur due to filtration. A dispersive mixing model would require that the deeper waters in the Milk River aquifer are remnants of a nonmarine water of unknown origin.

Ion Geochemistry

Nearly all ground water originates as rain or snow, which percolates through the soil into the underlying geologic zones. As the water moves through the soil zone and deeper into the ground-water system, its chemical characteristics are altered by a variety of geochemical processes. In the study area, recharge to the Milk River aquifer enters the sandstone both at outcrops and after passage through the soil and underlying formations. Most rock in the study area is overlain by glacial till.

Changes in the water chemistry can be shown graphically as percentages of total cation and anion concentrations by methods popularized by Piper (1944). Figure 26 shows the results of chemical analyses of typical sea water, fresh-stream water as it crosses the Milk River sandstone outcrop in the southern portion of the study area, and water from several wells tapping the Milk River aquifer. The sampling sites chosen for this figure are on a north-south line through the center of the study area and parallel to the direction of ground-water flow. The ground water flows due north from the outcrops areas several kilometers south of the United States–Canada border to about 100 km north of the border.

Freeze and Cherry (1979, p. 284) described three types of water in glacial deposits in North America. The water that occurs extensively in the interior plains region of the United States and Canada is called Type III water and is described by them as being typically "slightly alkaline, brackish water ($\approx$ 1000 to 10,000 mg/L TDS), in which Na^{+}, Mg^{2+}, Ca^{2+}, HCO_3^{-}, and SO_4^{2-} generally occur in major concentrations. Most of this water has SO_4^{2-} as the dominant anion." The description closely resembles the description of drift waters in the Foremost area given by Borneuf (1976, pp. 13-14). Percolation of fresh water through the glacial debris and into the Milk River sandstone would explain the high concentrations of sodium, magnesium, calcium, sulfate, bicarbonate, and total dissolved solids in sample 45, which was taken from the well closest to the sandstone outcrop in the Sweet Grass Hills. The high concentrations of sulfate, sodium, and total dissolved solids in T. 1 N., R. 13 W. (see figs. 14, 16, and 19)

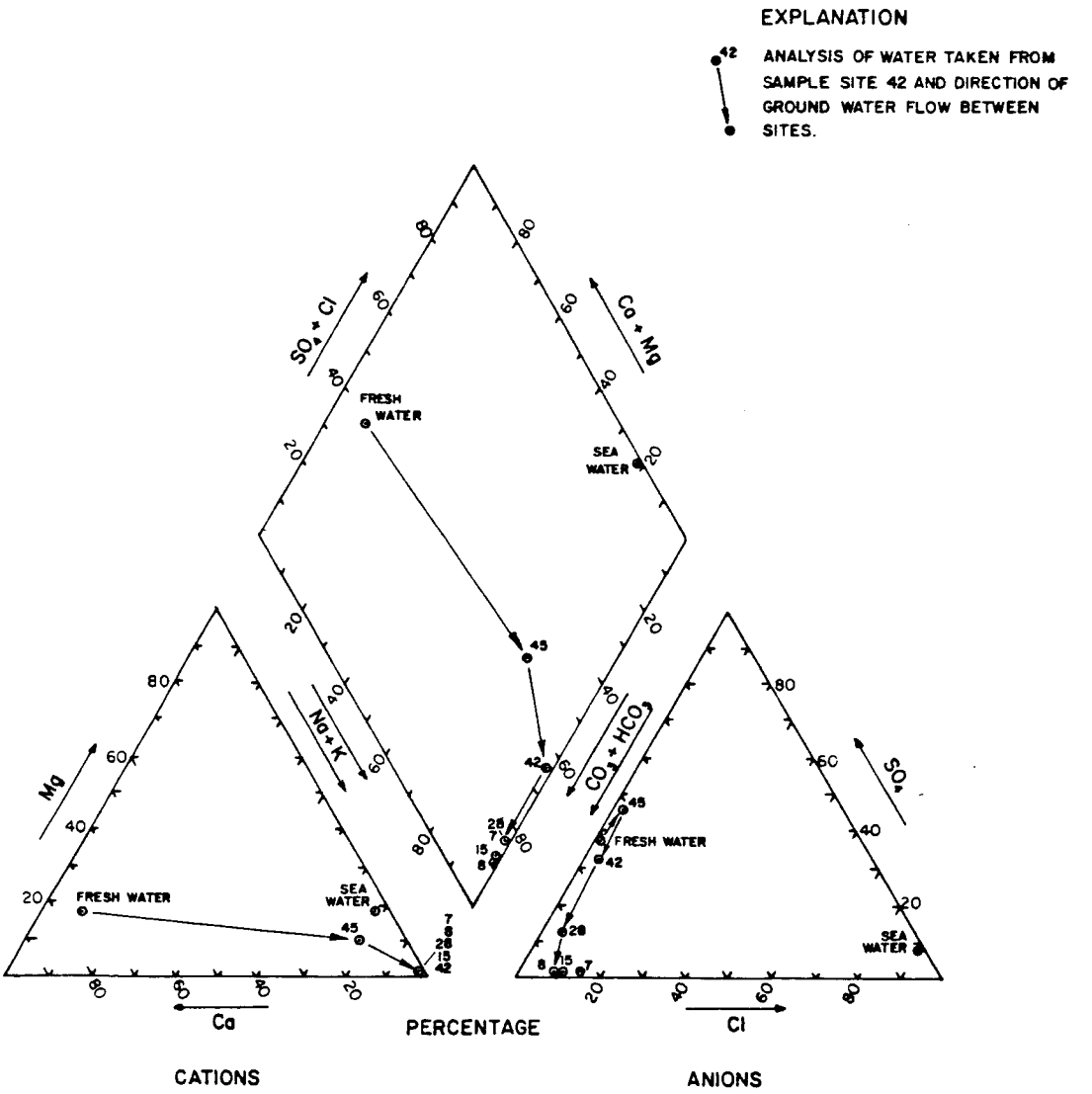

Figure 26. Chemical analyses of typical sea water, fresh stream water in the study area, and water from the Milk River aquifer.

Values shown as percentages of total equivalents per liter.

might be indicative of local recharge to the Milk River sandstone from glacial-drift waters in that area.

As the water moves downgradient from the area of recharge, calcium, magnesium, and sulfate concentrations decrease and sodium, chloride, and bicarbonate increase. Noticeable amounts of methane are also present in downgradient wells. The occurrence of sodium and bicarbonate as the dominant ions can be explained by the combined effects of calcite dissolution (from the sandstone cement) and ion exchange on clays. These processes can be represented as:

$$H_2CO_3 + CaCO_3 \rightarrow 2HCO_3^- + Ca^{2+}$$

$$Ca^{2+} + 2NaX \rightleftarrows 2Na^+ + Ca2X$$

where X denotes the clay particle to which the cation adsorbs. The slight decrease in magnesium concentration can also be attributed to cation exchange. The removal of calcium ion causes the system to be undersaturated with calcite, thereby allowing increased dissolution of calcite. The dissolution of calcite consumes carbon dioxide and produces increased amounts of sodium and bicarbonate and an increase in pH. A second mechanism that would cause an increase in bicarbonate ion concentration could be oxidation of organic matter by sulfate:

$$2CH_2O + SO_4^{2-} \rightarrow HCO_3^- + HS^- + CO_2 + H_2O$$

This mechanism would explain the decrease in sulfate downgradient from the recharge area. The required source of organic matter is abundant in the sandstone in the form of coal and peat. The "rotten-egg" odor

of H_2S at wells as noted during sample collection would support this hypothesis. The HS^- may also be lost to pyrite deposition.

An interpretation of Figure 26 lends further support to the two proposed mechanisms (cation exchange on clays and sulfate reduction) dominating the chemistry of the formation waters. According to Piper (1944), the processes of sulfate reduction and cation exchange would be traced on the trilinear diagram by straight-line vectors parallel to the bases of the central field (fig. 27). Samples from the study area seem to have two dominant trends. The first trend, as shown by the vector from the fresh-water sample to sample 42 in figure 26, suggests the dominant mechanism is exchange of sodium and potassium for calcium and magnesium. The second trend, as described by the vector from sample 42 to samples 28 and 15 in figure 26, suggests that the dominant mechanism is sulfate reduction.

Methane was observed bubbling in the water in many of the sampled wells. Figure 25 shows the sample locations where methane was observed. Also indicated on the figure are all sites at which no gas was noted. Because direct observation of the well water was sometimes not possible, the presence or absence of methane was not noted in many wells. There are two possible source of methane in the aquifer: biogenic and thermocatalytic. Biogenic methane is produced by methanogens (methane-producing bacteria) where associated bacteria maintain a low Eh. Thermocatalytic methane is generated during the thermal decomposition of organic matter during burial and diagenesis (Barker, Fritz, and Brown, 1978). Because of the fairly low ground-water

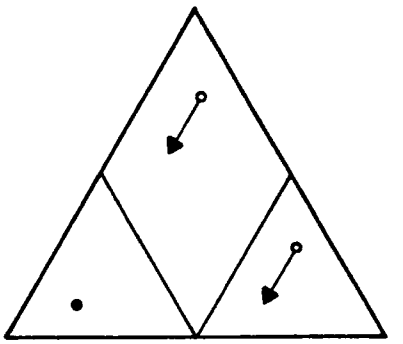

Reduction of Sulfate

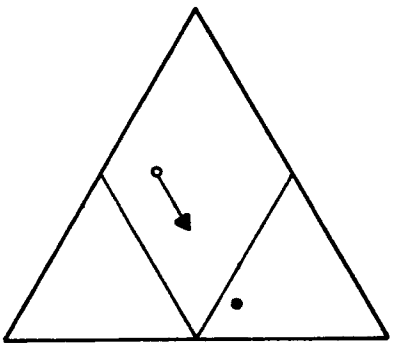

Base-exchange Softening

Figure 27. Vectors characteristic of geochemical process. -- After Piper (1944)

temperatures ($\sim$ 10°C) and the shallow depths ($<$ 900 ft) in the Milk River sandstone, the methane is probably biogenic.

It is commonly observed that methanogenesis occurs only in sulfate-depleted environments. Methane production is apparently inhibited by sulfate-reducing bacteria because methanogens cannot compete with sulfate reducers for H_2, a strong reducing agent. In this study, all sites with observed methane, except site 28, had sulfate concentrations of less than 10 mg/L.

Schoell (1980) suggested that biogenic methane is predominantly formed by bacterial reduction of CO_2:

$$CO_2 + 4H_2 \rightarrow CH_4 + 2H_2O$$

The hydrogen used would be formed from intermediate substances such as pyruvate, formate, hypoxanthine, and reduced pyridine nucleotides (Schoell, 1980). For this reaction to occur, there must be a source of carbon dioxide. Bicarbonate species provide such a source; also, Winograd and Farlekas (1974) suggested that lignite coalification,

$$C_nH_2O \rightarrow \frac{n}{2} CO_2\ (g) + \tfrac{1}{2}\ C_2H_{2n+2},$$

is an important source of CO_2 in some ground-water zones in the Atlantic and Gulf coastal plains. Lignite is available in the Milk River sandstone, and the required anaerobic conditions are present for such a reaction to occur.

GROUND-WATER AGES

Two methods were used to calculate the age of the water in the Milk River sandstone. A digital computer model using fluid-flow equations was used to calculate the hydrodynamic age profile. Carbon isotope concentration in water samples from the aquifer were analyzed and used to calculate carbon-14 ages at the sites. This chapter describes the models and input data and discusses the results.

Hydrodynamic Ages Based on a Steady-state Flow Model

Hydrodynamic age of ground water is the age determined from fluid-flow equations. Age of the water is the average amount of time it took the water to move from the surface of the earth to its position in the subsurface at the time of age determination. The digital computer model, WADAMO, developed by Brinkman (1982), was used to calculate the hydrodynamic age profile of the water in the Milk River aquifer. WADAMO is a quasi-three-dimensional, steady-state, finite-difference model, which calculates the historic steady-state potentiometric surface of the aquifer and then traces the flow path of the water up the hydraulic gradient to an internal source or to the edge of the nodal grid used to describe the area. Darcy's law is used to calculate the travel time along the flow path from one grid line to the next; the age of the water is the sum of the times between grid lines from a given position in the aquifer to its internal source or to the edge of the grid.

In the model WADAMO, a central aquifer, represented as a two-dimensional rectangular grid, is overlain and underlain by aquitards through which vertical leakage can occur. All interior nodes in the central aquifer are assigned values of horizontal permeability, porosity, and thickness. Each node is assigned values of vertical permeability for the aquitards above and below the central aquifer and values of potentiometric head in aquifers overlying and underlying the two aquitards. All boundary nodes, except the four corner nodes, and any desired interior nodes are assigned constant head or constant-flux values.

The major assumptions for WADAMO are:

1. The aquifer is isotropic with respect to permeability.
2. Flow in the central aquifer is horizontal.
3. Flow through the overlying and underlying aquitards is vertical.
4. Parameter values relating to flow in the central aquifer vary linearly between adjacent nodes.
5. In unconfined areas of the aquifer, transmissivity does not change with changes in saturated thickness.
6. Dispersion is negligible.

The equation of continuity of mass and Darcy's law are used in the model to calculate heads in the central aquifer. These calculated heads are compared to the calculated heads from the last iteration, and if a given error tolerance between the two is met, the heads are assumed to represent steady-state conditions. If the error is greater

than the given error tolerance, another iteration will be run. During each successive iteration, the value of hydraulic head at each interior node is better approximated by use of a convergence routine. These iterations continue until the error criterion is met. Once steady state is achieved, these heads are used to determine travel times for the movement of the ground water. The ages are determined from a form of Darcy's law by tracing the flow from any node up hydraulic gradient to either the internal source or a boundary node.

Output from WADAMO indicates the source area for the water at each node, telling whether the flow came from an internal source node or from a boundary node. If the water enters the modeled area through a boundary , the boundary from which the flow came is indicated. The usefulness of this feature will become more obvious in the following discussion of the results of modeling. The reader is referred to Brinkman (1982) for further details on the mathematical arguments and operation of the model.

Meyboom (1960, p. 41-43) described the Milk River aquifer as being in a state of dynamic equilibrium prior to disturbance by the downcutting of the Milk River during postglacial time. When the Milk River cut its present valley, it intersected the Milk River aquifer and greatly increased the natural discharge of the system by means of springs and seeps from sandstone outcrops along the river. The postglacial disturbance was followed by an adjustment of the hydraulic system to a new dynamic equilibrium. The discharge along the river would have caused a steepening of the hydraulic gradient between the Milk River and the Milk River sandstone outcrops to the south. It would

probably have been accompanied by a lowering of the potentiometric surface over a broad area. In this thesis, the Milk River aquifer and related hydraulic system were modeled so as to calculate the steady-state heads as they would have been prior to the downcutting of the Milk River.

The grid for the model was 41 nodes north-south by 35 nodes east-west, covering an area of about 66 miles by 48 miles (fig. 28). The western boundary is a north-south line through Pakowki Lake; the northern boundary is an east-west line through the town of Bow Island; and the southern boundary is an east-west line 6 miles south of and parallel to the international border.

The system was modeled with the Milk River sandstone as the central aquifer, overlain by an confining bed formed by the clays and shales of the Pakowki, Foremost, and Oldman formations and underlain by a confining bed formed by the shales and clays of the Colorado formation. The water table in the surficial deposits and the potentiometric surface of the Bow Island formation, which are above and below the described three-layer system, respectively, were input to the model for determination of vertical leakage into and out of the central aquifer. The northern, eastern, and western boundary nodes were assigned constant fluxes. Near the southern boundary, nodes that approximated the outcrop areas of the Milk River sandstone were assigned constant head values. Any nodes south of the outcrop were assigned very low values of constant heads to assure that they would not artificially influence flow in the model. More detail on the selection and reliability of the model parameters is given in Appendix C.

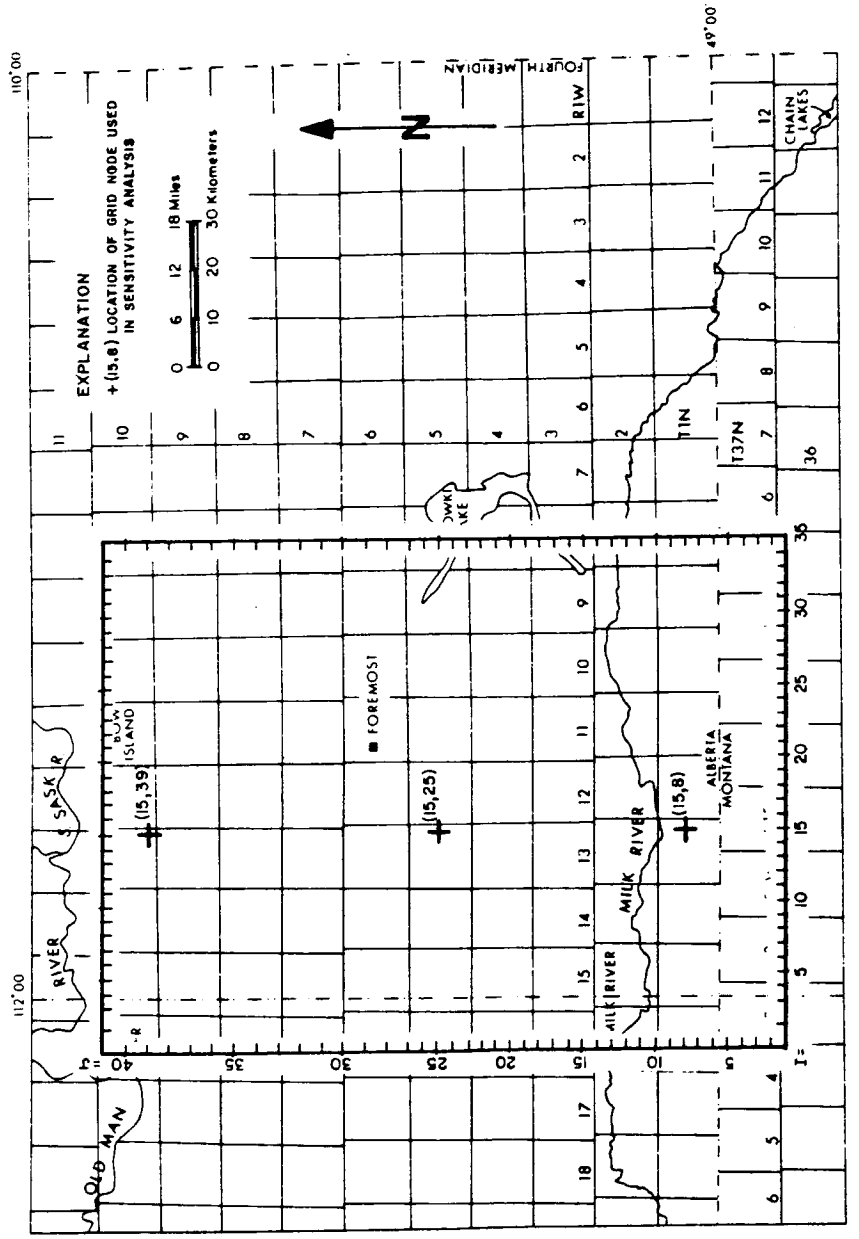

Figure 28. Nodal grid in WADAMO

Model Input

A set of standard values was determined for each node in the model grid. The grid was overlaid on various contour maps and the most representative value for each grid node was chosen as the standard value. Standard values of Milk River aquifer transmissivity and thickness were taken from figures 9 and 10, respectively. The aquitard thickness contours that represent standard values above and below the central aquifer are shown in figures 29 and 30. Standard values for the driving heads above the Milk River aquifer were taken from the water-table contours of the surficial deposits (fig. 7), and standard values of driving heads beneath the Milk River aquifer were taken from figure 11, which shows the potentiometric surface of the Bow Island sandstone. Description of the source for standard values of constant fluxes and constant heads can be found in Appendix C. A standard value for the porosity of the Milk River aquifer (10%) was taken from Meyboom (1960). The vertical permeabilities of the shales and clays that form the aquitards above and below the Milk River aquifer are not reported in the literature. To determine standard values for vertical permeability, the heads in the Milk River aquifer along the northern grid boundary were assumed not to have been significantly affected by downcutting of the Milk River. The permeability of each aquitard was also assumed to be areally constant and the permeability of the upper aquitard to be twice that of the lower aquitard. The reasoning behind the last assumption is explained in Appendix C. The model was run with standard values for all parameters except vertical permeabilities, which were increased by 50 percent for each successive

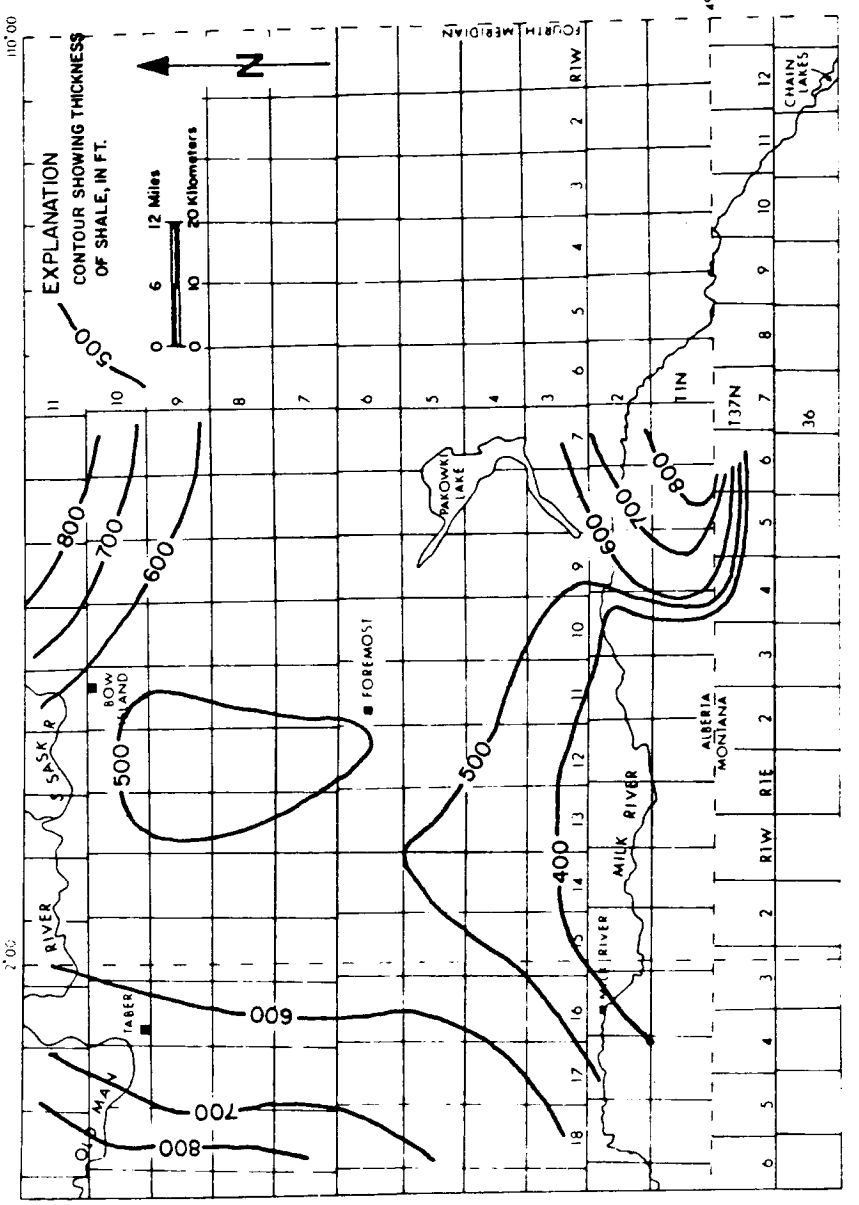

Figure 29. Isopach of the shale beds above the Milk River aquifer

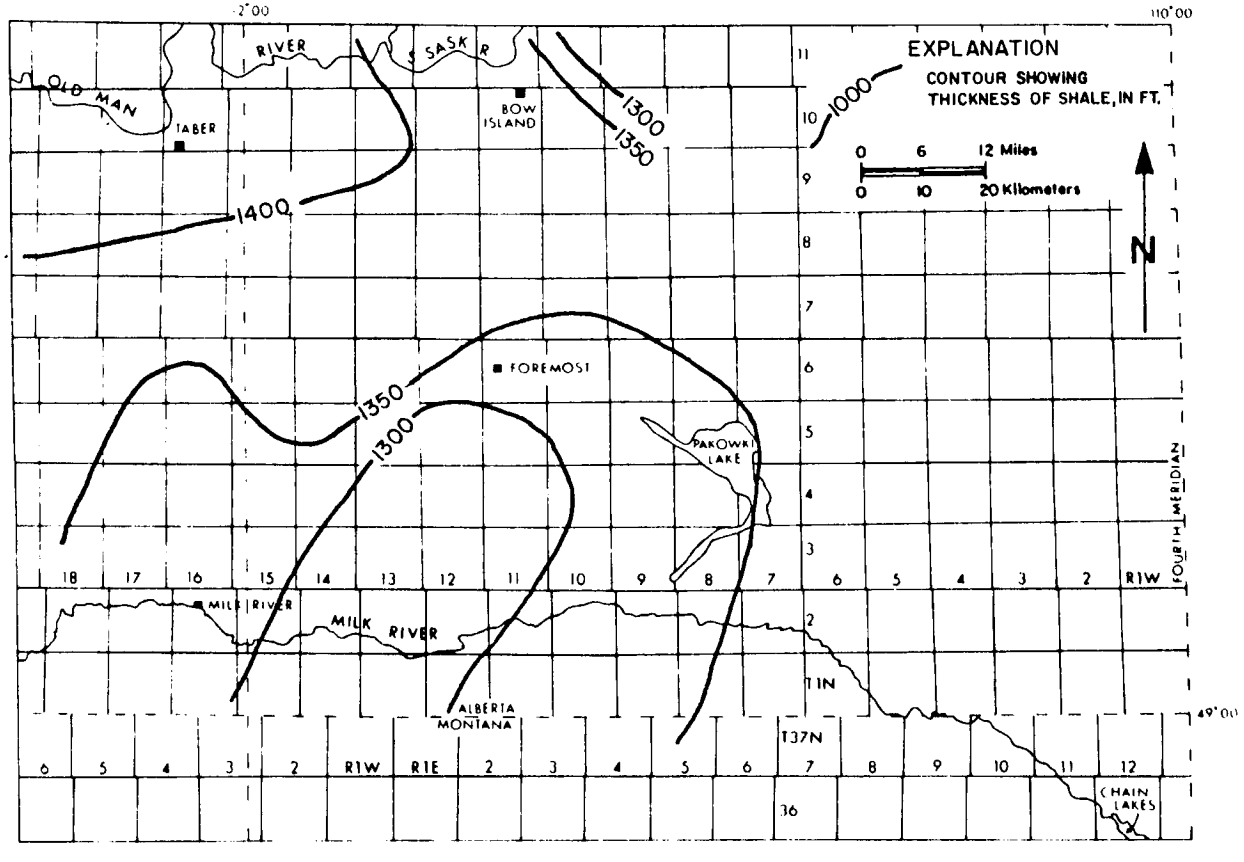

Figure 30. Isopach of the shale beds below the Milk River aquifer

run. The vertical permeabilities from the model run that best duplicated the heads along the northern boundary were chosen as standard values. Those standard values for aquitard permeabilities were 5×10^{-7} gpd/ft^2 for the aquitard above and 2.5×10^{-7} gpd/ft^2 for the aquitard below the Milk River aquifer.

Model Output

The heads in the Milk River aquifer and the ages of the water as predicted by the model run with standard values for all parameters are shown in figures 31 and 32. Ages in the eastern and northeastern parts of the study area are not shown in figure 32 because the model output indicated that the water at those nodes came from the eastern grid boundary. The age predicted for those nodes are representative of only the time of travel from the eastern boundary not from any recharge source. The model predicted ages that ranged from zero years in the area of sandstone outcrop in the Sweet Grass Hills to about 500,000 years in the northwestern corner of the study area. The model also predicted heads near the Milk River that are about 200 to 300 feet higher than they were in 1958 (compare figs. 31 and 8). This difference in heads would suggest that downcutting of the overlying shales and clays by the Milk River during postglacial times caused a reversal of flow direction of water in the aquifer north of the river for some period of time prior to re-equilibration of the system. It would also suggest that the hydraulic gradient south of the Milk River has been increased about 40 to 50 percent since Wisconsin time. Because of the increased gradient, ages today should be younger than those

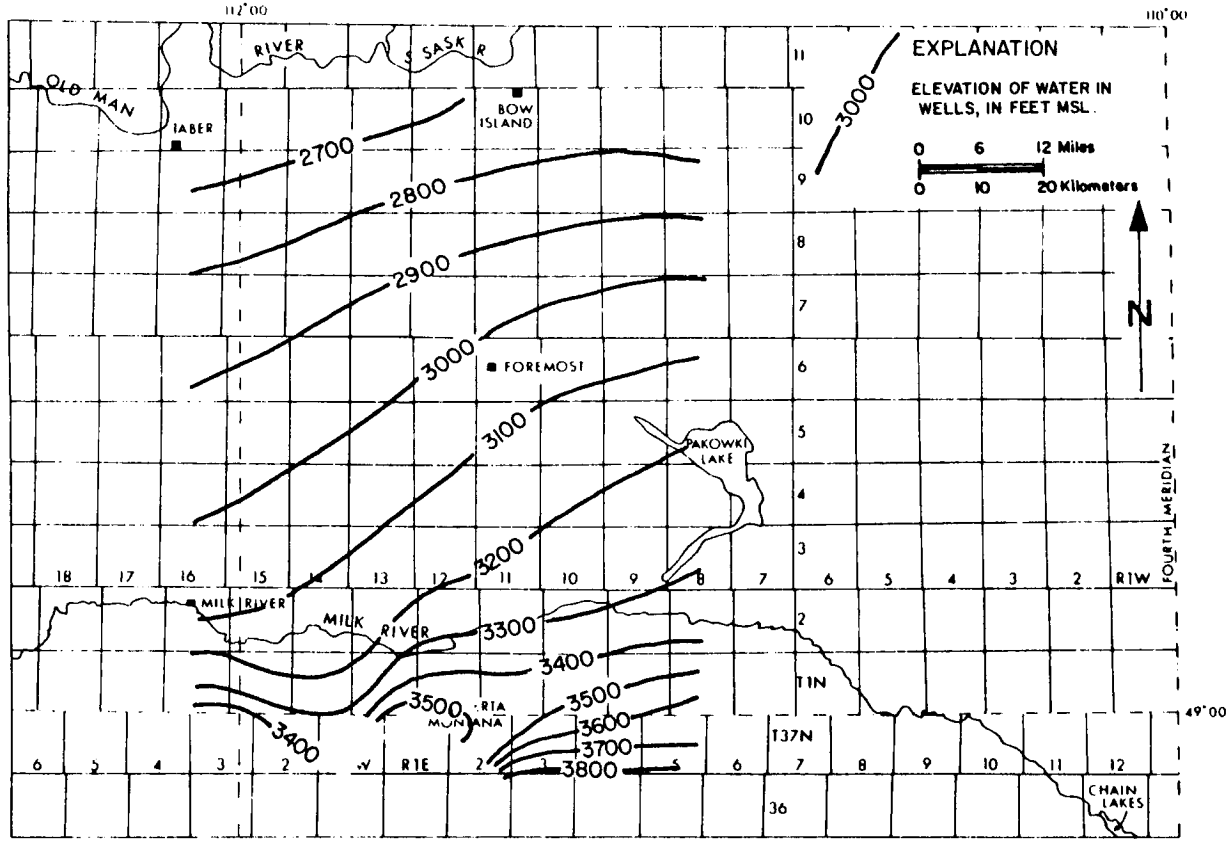

Figure 31. Steady-state potentiometric heads in the Milk River aquifer prior to downcutting by the Milk River

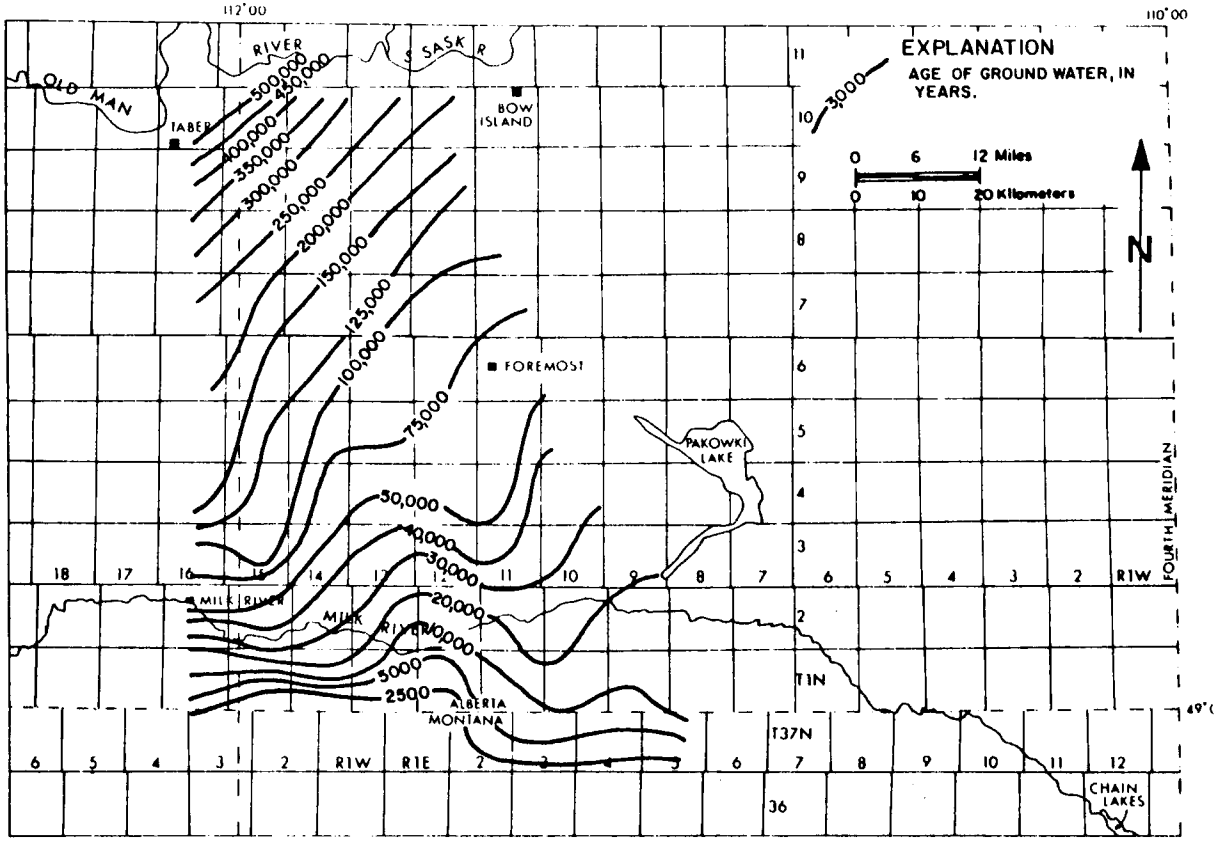

Figure 32. Age contours of water in the Milk River aquifer based on steady-state potentiometric heads prior to downcutting of the Milk River

predicted by the model for areas between the sandstone outcrop and the Milk River.

Sensitivity Analysis

The modeled system was analyzed for its sensitivity to changes of the various input parameters. The output steady-state heads and ages were then compared to those predicted using only the standard values. For each calculation, only one of the parameters was varied from its standard value and all other parameters were left unchanged. Table 1 shows the changes in steady-state head and ages for each of three aquifer nodes, which were chosen to represent changes occurring along a north-south center line at the south end (node 15,8), center (node 15,25), and north end (node 15,39) of the study area. (See figure 23 for node locations.)

Runs 1 and 2 show that a 50 percent increase or decrease in the flux across the north boundary causes only a very minor change ($< 1\%$) in the predicted ages throughout the south and central parts of the study area and small changes ($\leq 8\%$) in ages very near the north boundary. An increase in the north flux caused a decrease in all predicted ages, and a decrease caused an increase in the predicted ages.

Run 3 shows that decreasing the constant heads along the recharged area (south boundary) by 100 feet caused a 9.49 percent increase in ages near the south boundary, but only a 5.03 percent increase in age in the north. No sensitivity analysis was run for an increase in constant heads along the recharge area because the

Table 1. Variation of heads and ages due to changes in input parameters from standard values

	Run				
	1	2	3	4	5
Change from standard value of flux on northern boundary (percent)	50	-50	X	X	X
Change from standard value of constant head on south boundary (feet)	X	X	-100	X	X
Change from standard value of vertical permeability for upper and lower aquitards (percent)	X	X	X	-33	50
Change in steady-state head (feet)					
South[1]	-1	1	-64	32	-35
Central[2]	-4	5	-23	94	-87
North[2]	-20	29	-12	112	-93
Change in age (percent)					
South[1]	-0.23	0.23	9.49	8.17	22.7
Central[2]	-0.02	0.05	8.82	6.10	2.75
North[3]	-6.66	8.00	5.03	7.90	-2.90

1. Calculated for grid node (15,8).
2. Calculated for grid node (15,25).
3. Calculated for grid node (15,39).

standard value heads are so near land surface that an increase of 50 to 100 feet would bring them above land surface.

Runs 4 and 5 show the effects of varying the vertical permeabilities of the aquitards by -33 and 50 percent, respectively. A decrease in vertical permeability resulted in an increase in age of about 7 percent over the entire aquifer. An increase in vertical permeability caused the ages to increase in the south by about 22 percent and decrease in the north by about 3 percent.

The values of porosity and transmissivity of the central aquifer were not varied for the sensitivity analysis. Changes in porosity directly affect the hydrodynamic ages; doubling porosity causes the age to double. Although transmissivity was not varied, its effects on the ages are probably small. Brinkman (1982, Table II) found in a similar sensitivity analysis that by varying transmissivity 10 to 20 percent, the ages changed only a fraction of a percentage point.

Discussion of Results

The model output and sensitivity analysis indicate that the predicted ground-water ages are most sensitive to changes in porosity and vertical permeability. These two parameters happen to be the least documented parameters in the hydrologic system associated with the Milk River aquifer.

Porosity values in sandstones are commonly in the range of 10 to 20 percent (Davis, 1969, p. 72). Thornstenson, Fisher, and Croft (1979) measured total porosities of 31 to 38 percent for sandstones in the Fox Hills–basal Hell Creek aquifer in North Dakota, and Meijer-

Drees (1973) reported porosities of 17.3 to 26.0 percent in clean, well-sorted silt lenses in the Milk River formation just north of the study area. These findings indicate that the standard value of porosity (10%) for the Milk River formation may be too low.

Vertical permeabilities of shales and clays have been reported by many investigators, including Davis and DeWeist (1967) and Young, Low, and McLatchie (1964). Davis and DeWeist (1967, p. 349) reported shale permeabilities of 9×10^{-5} and 4×10^{-3} md (millidarcy) [$\sim 1.6 \times 10^{-6}$ and 7.2×10^{-5} gpd/ft^2(gallons per day per square foot)]. Young and others (1964) measured permeabilities of argillaceous rocks from the Lower Cretaceous strata of western Canada ranging from 10^{-7} to 10^{-4} md ($\sim 1{,}8 \times 10^{-9}$ to 1.8×10^{-6} gpd/ft^2). These permeabilities indicate that shale permeabilities vary greatly. The standard values used in the model may be increased or decreased by about two orders of magnitude and remain in the range of reasonable values.

Ages as Determined by Carbon Isotope Methods

Since the 1950s, naturally occurring carbon isotopes that exist in water in the hydrologic cycle have been used in the investigations of ground water. Prior to 1953, ^{14}C, a radioactive isotope of carbon, was derived almost entirely by cosmogenic neutrons activating ^{14}N atoms in the upper atmosphere. Above-ground thermonuclear tests, which began in 1953, significantly increased the ^{14}C production to levels above the natural background level of 2.5 atoms/s$\cdot$cm^2 (Freeze and Cherry, 1979). The carbon atom formed is oxidized to CO_2 and is then mixed with the atmospheric CO_2 reservoir.

When water is exposed to the CO_2, the gas and water will mix and the carbonate components in the water (CO_2, H_2CO_3, HCO_3^-, and CO_3^{2-}) will have ^{14}C concentrations based on equilibrium conditions between the CO_2 gas and the water. When the water moves below the water table and becomes isolated from the earth's CO_2 reservoir in the atmosphere and soil zone, radioactive decay causes the ^{14}C content in the dissolved carbon to gradually decline.

For any kind of radiochronometry technique, the time elapsed in a reservoir is given by the general equation of radioactive decay:

$$t = - \frac{\tau}{\log 2} \log \frac{A}{A_o}$$

where τ is the half-life of the isotope, A is the level of radioactivity after time t, and A_o is the initial radioactive at some initial time. The above equation can be rearranged, and upon substitution of τ = 5,730 years (the half-life of ^{14}C) yields

$$t = -8{,}270 \ln \frac{A}{A_o}$$

Most ground water has a total dissolved carbon content of composite origin caused by: (1) exposure to the earth's atmosphere prior to infiltration into the subsurface environment, (2) contact with soil gases during infiltration through the unsaturated zone, and (3) gas production below the water table by chemical or biochemical reactions involving the ground water, minerals, organic matter, and bacterial activity. Any addition to or loss of carbon from the water after it has equilibrated with the soil CO_2 will cause a change in the concentration

of ^{14}C of the total dissolved carbon, thus causing a divergence between the real age of the water (the time elapsed since the water moved deep enough into the ground-water zone to become isolated from the earth's atmosphere) and the apparent age of the dissolved inorganic carbon. To obtain ^{14}C estimates of the actual ground-water age it is necessary to determine the extent to which "dead" carbon has reduced the relative ^{14}C content of the ground water.

Inorganic carbon that enters the water by mineral dissolution above the water table is assumed to have little influence on the ^{14}C content of the water because of rapid equilibration with the ^{14}C in the soil air, which has ^{14}C at modern levels. If carbonate–mineral dissolution takes place in the unsaturated zone, sufficient CO_2 is usually generated by decay of organic matter to maintain equilibrium of ^{14}C contents between the water and the soil atmosphere. Whether the organic matter in the soil is tens of years old or a few hundreds of years old is of little consequence, because these time period are short relative to the half-life of ^{14}C. It is also assumed that the fraction of the total dissolved inorganic carbon derived below the water table by mineral dissolution or oxidation of organic matter contains no ^{14}C (Freeze and Cherry, 1979).

As ground water evolves chemically along its flow path, the fraction of contributed total inorganic carbon can increase or decrease. Therefore, to make an estimate of the true age of the water from ^{14}C data, a detailed understanding of the geochemical origin of the inorganic carbon in the ground water is necessary. Conceptual geochemical models have been developed and improved that use analyses of ^{13}C, a

nonradioactive isotope of carbon. Fontes and Garnier (1979) reviewed the existing models for determining the initial ^{14}C activity of the total dissolved carbon and presented a new approach. Each model reviewed by Fontes and Garnier dealt only with inorganic sources of carbon. The models do not take into account any organically derived carbon after the water has moved below the zone where it is exposed to the atmosphere.

The addition of carbon from organic sources has been recognized by Winograd and Farlekas (1974), Plummer (1977), and Barker and others (1978) among others. Winograd and Farlekas (1974) suggested that coalification of ubiquitous lignitic detritus was the source of the CO_2 generated in the Potomoc–Raritan–Magothy aquifer system to distances of 45 km down hydraulic gradient from the aquifer outcrop area. Plummer (1977) found that oxidation of lignite by means of sulfate reduction added additional carbon to the ground water in the Floridan aquifer and corrected the ^{14}C ages using derived mass transfer reactions. Barker and others (1978) found that ground waters containing significant biogenic methane had abnormally heavy $\delta^{13}C$ values for the total dissolved inorganic carbon and developed conceptual models to adjust the ^{14}C activity of the ground water for the effects of methanogenesis and for dilution of the carbon present during infiltration by simple dissolution of rock carbonate.

In my study, only 3 of the 12 sites where carbon isotope concentrations in the ground water were analyzed are relatively unaffected by sulfate reduction and biogenic methanogenesis. These sites were 45, 41, and 42, in order of increasing distance from the sandstone outcrop.

Because the models used to adjust for the effects of sulfate reduction and biogenic methanogenesis are complex and beyond the scope of this work, ^{14}C ages were calculated only for the areas unaffected by these chemical reactions.

Determination of the Initial Activity of Dissolved Carbon

Two methods of estimating A_o, the initial activity of the dissolved carbon in the water, were used in this study. Tamers (1975) proposed a method that assumes perfect stoichiometry for the various chemical reactions involving carbon and does not consider isotope exchange. If the soil carbonates have a ^{14}C activity equal to zero, then in the normal range of pH values in ground waters, the dilution of active carbon in the total dissolved carbon content of a sample can be expressed as

$$A_o = \frac{m\ CO_2 + 0.5\ m\ HCO_3^-}{m\ CO_2 + m\ HCO_3^-} A_g$$

where m stands for molalities and A_g is the ^{14}C activity of the soil CO_2 (generally taken as 100% modern carbon).

Fontes and Garnier (1979) proposed a model that accounted for carbon chemistry in terms of mixing of different components and for isotope fractionation effects during exchange reactions within the aquifer. The initial activity of the total dissolved carbon prior to any radioactive decay can be expressed as

$$A_o = [1 - \frac{C_m}{C_t}A_g + \frac{C_m}{C_t}A_m] + [(A_g - 0.2\varepsilon - A_m)$$

$$\times \frac{\delta_t - (C_m/C_t)\delta_m - [1 - (C_m/C_t)]\delta_g}{\delta_g - \varepsilon - \delta_m}]$$

where C_m = molal concentration of dissolved carbon coming from solid carbonates

C_t = molal concentration of total dissolved inorganic carbon

A_m = ^{14}C content as percent modern carbon of the solid carbon

A_g = ^{14}C content as percent modern carbon (pmc) of the gaseous carbon

ε = isotope enrichment factor, per mille, at equilibrium between CO_2 and solid carbonate

δ_t = measured per mille $\delta^{13}C$ value of ground-water sample

δ_m = per mille $\delta^{13}C$ of solid carbonate

δ_g = per mille $\delta^{13}C$ value of the gaseous carbon

Table 2 shows the input parameters used in the two models and Table 3 shows the calculated ages of the water at each site.

The $\delta^{13}C$ values of solid carbonates from soil and from aquifer (δ_m in the Fontes and Garnier model) are generally close to zero if they are from marine origin. Because δ_m was not measured for this study, a range of values from -2 to +2 percent was used.

The major sources of CO_2 in the soil are from decomposition of organic matter, plant-root respiration, and atmospheric CO_2. The $\delta^{13}C$ content of the gaseous soil CO_2 depends mostly on the vegetation in the

Table 2. Factors used in determining initial ^{14}C activity of total dissolved carbon

	Sample		
	45	41	42
pH[a]	7.46	8.83	8.74
HCO_3^{-1} (mmol)	8.61	8.80	9.61
CO_2 (aq) (mmol)[b]	0.25	0.01	0.01
C_m (mmol)	4.30	5.30	6.40
C_t (mmol)	9.48	9.74	11.26
ε (‰)[c]	-11.55	-11.08	-11.43
A_m (pmc)	0	0	0
A_g (pmc)	100	100	100
δ_m (‰)	-2 to +2	-2 to +2	-2 to +2
δ_g (‰)	-24 to -20	-24 to -20	-24 to -20
δ_t (‰)	-12.6	-13.4	-13.6

a. Measurements were performed during sample collection.

b. Calculated based on carbonate chemistry of sample being in equilibrium at 8°C (Stumm and Morgan, 1970, p. 55):

$$[CO_2 \text{ (aq)}] = [H^+]\ [HCO_3^-]\ 10^{5.93}.$$

c. Isotope enrichment factor between gaseous CO_2 and solid carbonate (after Fontes and Garnier, 1979):

$$\varepsilon \sim -12.38 + 0.10t, \text{ where } t = \text{temperature in °C}.$$

Table 3. Calculated values of initial ^{14}C activity of total dissolved carbon and adjusted ages of water

	Sample		
	1	2	3
Tamers Model			
A_o (pmc)	51.4	50.1	50.1
Age (years B.P.)	5,670	15,699	28,474
Fontes and Garnier Model			
A_o (pmc)	40.7 to 80.0	59.1 to 98.4	54.1 to 93.3
Age (years B.P.)	3,744 to 9,315	15,493 to 20,200	28,559 to 33,260
A (pmc)	25.9 ± 0.5	7.5 ± 0.6	1.6 ± 0.1

recharge area at the time the sample entered the aquifer. Most vegetation has $\delta^{13}C$ values averaging about -25 $^{o}/_{oo}$, and similarly low values can be expected for CO_2 from organic decay and plant respiration (Deines, Langmuir, and Harmon, 1974). Pearson and Hanshaw (1970) found that for soils in arid to semiarid climates where plant activity is very much reduced, heavier $\delta^{13}C$ values can be expected. In their work, they found that some arid West Texas soils had $\delta^{13}C$ values between -15 and -19 $^{o}/_{oo}$. Because the $\delta^{13}C$ of the soil CO_2 was not measured for this study, estimates were based on published values from other regions. Because the Sweet Grass Hills area is semiarid and has sparse vegetation near the Milk River sandstone outcrop, the $\delta^{13}C$ in the soil CO_2 may be slightly greater than -25 $^{o}/_{oo}$. Initially, a range of values of -18 to -24 percent was used in the Fontes and Garnier (1979) model, but use of δ^{13} = -18% yielded initial ^{14}C activities in excess of 100 percent. The upper value used for the model was therefore decreased from -18 to -20 $^{o}/_{oo}$.

The initial activity of the carbon in the soil gas was assumed to be 100 pmc, and the aquifer carbonates (solid) were assumed to be "dead"; i.e., their activities were zero pmc.

Discussion of Results

The adjusted ages of the ground water for sites 45, 41, and 42 are given in table 3. The ages at the three sites are about 6,000, 18,000, and 30,000, respectively. The ages predicted by the hydrodynamic model (fig. 32) are about 4,000, 15,000, and 25,000, respectively: about 20 percent younger than the carbon ages.

As discussed previously, the hydraulic gradient between the recharge zone and the Milk River aquifer may have increased by about 40 to 50 percent since the downcutting into the Milk River sandstone by the Milk River. This increase in hydraulic gradient would be accompanied by ground water moving at greater velocities; therefore, the water at each of the three sites would be expected to be younger today than prior to downcutting. A 50 percent increase in hydraulic gradient since downcutting would cause the carbon ages to be about two-thirds the modeled hydrodynamic ages. (Age is inversely proportional to hydraulic gradient; therefore, an increase of gradient by 3/2 causes a decrease in age to 2/3 its original value, which is not the finding from the models used in this study.)

Several explanations for the discrepancy between expected and predicted ages are possible. The value of A_o in the carbon models is highly uncertain, which could cause inaccuracy in the carbon ages. But even the lowest values of A_o from table 3 yield calculated ages of 3,744, 15,493, and 28,474 years at sites 45, 41, and 42, respectively, which only reduces the carbon ages to values approximately equal to the hydrodynamic ages. An increase of the predicted hydrodynamic ages can occur through variation of the input parameters to WADAMO. The model is sensitive to changes in the constant heads in the recharge zone, the porosity, and the vertical permeability. Changes in any of these parameters individually or together could produce an increase in ages to the expected levels of about 50 percent higher than those of the steady-state hydrodynamic heads.

An age profile developed with results from ^{36}Cl analysis (Bentley, 1982) revealed a similar profile but significantly different ages at each location in the aquifer. The ground water was estimated to be about three or four times as old by the chloride isotope method; in the far northern part of the study area, near Taber, the ^{36}Cl-predicted age was about 2 million years as opposed to the 500,000 years predicted by the flow model used in my study. Bentley is inclined to believe that the cause of the different ages predicted is due to the possibly improper assumption of a steady-state flow system in the Milk River aquifer (Bentley, 1982).

In my study no estimate was made of the effects of permafrost in the sandstone outcrop area or to the presence of glaciers over the sandstone outcrop on the predicted age of the water. Either phenomenon would probably decrease recharge, causing the ground water to move more slowly in the aquifer and thereby increasing the real ages relative to the predicted steady-state ages.

SUMMARY AND CONCLUSIONS

Most recharge to the Milk River aquifer occurs where the sandstone is exposed at land surface in the Sweet Grass Hills. The sandstone dips to the northeast and west from this outcrop area. The present-day potentiometric surface of the aquifer shows the water moving northward away from the outcrop area. Geochemical studies of the ground water reveal complex distributions of the ions and deuterium and ^{18}O, which can be explained by several processes. The geochemical evolution of the ground water is complicated by physical processes, probably either ion infiltration through shales and clays or by mixing of fresh recharge waters with deeper altered water in the aquifer.

A quasi-three-dimensional, steady-state, finite-difference computer program was used to model the Milk River aquifer system as it was prior to the incision of the Milk River into the Milk River sandstone during postglacial time. Results of the model indicate that the Milk River downcutting lowered the potentiometric heads of the Milk River aquifer by about 200 to 300 feet in the vicinity of the river. The model also predicted that the oldest waters in the aquifer are in the far northwest corner of the study area. These waters are about half a million years old.

Carbon modeling of the ground water shows it becoming progressively older northward from the Sweet Grass Hills. The ages predicted by this method are about 10 to 20 percent older than the ages predicted by the hydrodynamic model. Carbon modeling was not done

on samples north of the Milk River because sulfate reduction and methanogenesis in the aquifer contribute carbon to the ground water and complicate the models.

An interpretation of the results of the hydrodynamic modeling indicates that the ages predicted by that model should be about 40 to 50 percent older than the carbon-derived ages because of changes in the flow system due to downcutting of the Milk River during postglacial time. The discrepancy between the expected differences in age and the actual difference in age between the two models may be attributed to the differences between aquifer and confining-bed parameters in nature and those used in the hydrodynamic model. A sensitivity analysis of the aquifer parameters showed that variation of the vertical permeabilities in the confining beds, lowering the constant head boundary in the recharge area, or increasing the porosity of the Milk River sandstone could produce the expected ages from the hydrodynamic model.

APPENDIX A

FIELD PROCEDURES FOR COLLECTING CHLORINE AND CARBON FOR ISOTOPE ANALYSIS

Chlorine Samples

1. Rinse sampling container three times with sampling solution. Collect enough sample to produce about 100 mg of chloride. Place sample in black plastic sampling container.

2. Add enough concentrated HNO_3 to get the pH below 3.0.

3. Add enough $AgNO_3$ to precipitate three times the chloride in the sample.

4. Store in dark place for 8 hours.

5. Decant supernate. Pour precipitate into glass bottle.

6. Rinse barrel with reagent-grade NH_3OH.

Carbon Samples

1. Use polyethylene bottle large enough to hold the amount of sample water required to produce at least 2.0 g carbon. Rinse bottle three times with sample solution. Fill bottle to top.

2. Add enough NaOH to get pH greater than 11.2.

3. Add enough $BaCl_2$ to precipitate four times the amount of carbon in the sample.

4. Add agent to produce flocculation. Cap jug tightly and shake.

5. Allow to sit for 8 hours. Pour off supernate and store precipitate in 1-liter polyethylene bottle.

6. Rinse large sampling bottle several times with tap water.

APPENDIX B

ANALYTICAL RESULTS

Table B-1. Chemical analyses of samples from southeastern Alberta and northern Montana

Location (¼S,S,T,R,)	Sample Number	Temperature (°C)	Sodium (Na)	Potassium (K)	Magnesium (Mg)	Calcium (Ca)	Iron (Fe)	Total Dissolved Solids	Sulfate (SO_4)	Fluorinee (F)	Chlorine (Cl)	Bicarbonate (HCO_3)	Carbonate (CO_3)	pH	Remarks
SE-24-09-17	1	15.0	1000	2.2	1.2	2.2	0.2	2600	<2.0	2.7	627	1476	48	8.32	flowing well
SE-06-09-16	2	18.0	910	2.0	1.1	2.0	0.2	2400	<2.0	2.9	495	--	--	8.51	flowing well
SW-01-08-16	4	13.5	960	2.5	1.4	3.0	0.2	2600	7.0	2.6	610	1464	36	8.17	pumped well
SE-04-08-13	5	15.0	850	2.9	2.4	3.0	3.3	2400	5.3	2.8	402	--	--	--	pumped well
NW-22-09-13	6	18.2	550	1.5	0.5	1.2	0.1	1500	3.5	5.6	136	--	--	--	
NE-35-09-12	7	11.5	520	1.2	0.5	1.2	0.1	1400	4.2	3.6	130	939	114	8.75	flowing well
NE-26-08-12	8	11.5	440	1.1	0.3	0.9	0.1	1100	3.5	2.5	73	885	96	8.78	flowing well, sample taken after in-line pressure tank
SW-19-10-12	9	11.8	760	1.9	1.0	2.2	0.2	2000	2.8	4.6	181	1214	66	8.49	flowing well
NW-24-10-11	10	12.5	1300	3.4	3.2	6.2	0.4	3400	<2.0	1.1	1295	--	--	--	
NE-35-09-11	11	11.0	730	1.7	0.9	2.0	0.2	1900	<2.0	3.6	356	1122	66	8.37	flowing well
SE-35-08-11	12	12.1	460	1.3	0.5	1.2	0.7	1300	6.0	3.4	110	976	66	8.51	pumped well
NE-17-08-11	13	8.5	440	1.0	0.5	1.1	0.8	1200	6.3	1.8	92	854	90	8.72	pumped well
SE-08-07-11	14	9.8	550	1.9	5.4	7.6	2.6	1600	61	3.4	220	--	--	--	pumped wells, possible contamination due to collapsed casing

Table B-1--Continued

Location (#S,S,T,R,)	Sample Number	Temperature (°C)	Sodium (Na)	Potassium (K)	Magnesium (Mg)	Calcium (Ca)	Iron (Fe)	Total Dissolved Solids	Sulfate (SO_4)	Fluorinee (F)	Chlorine (Cl)	Bicarbonate (HCO_3)	Carbonate (CO_3)	pH	Remarks
SE-25-07-11	15	11.5	440	1.0	0.4	0.9	0.2	1200	3.4	2.2	82	878	108	8.79	pumped well
NE-09-07-10	16	10.0	440	1.1	0.5	0.9	0.2	1200	<2.0	2.1	80	781	96	8.75	pumped well
NE-23-09-09	17	9.5	1100	3.4	3.4	7.0	1.6	3100	12	0.9	1093	988	36	8.18	
SE-14-09-09	18	--	1100	3.2	2.8	5.6	0.3	3000	<2.0	1.0	1053	--	--	--	pumped well
NE-22-08-09	19	13.5	730	1.9	1.5	2.8	1.1	1900	2.2	2.7	434	1104	42	8.37	flowing well
NW-02-08-09	20	13.8	880	2.0	1.6	3.4	0.2	2300	<2.0	2.2	699	1007	42	8.28	pumped well
SE-27-07-09	21	11.6	780	1.9	1.2	2.2	0.1	2000	<2.0	1.8	453	--	--	--	pumped well
SW-12-06-09	22	12.0	440	1.1	0.5	1.5	0.4	1200	4.9	2.1	82	824	108	8.65	pumped well
NE-10-05-07	23	11.0	440	1.1	0.5	1.4	0.2	1200	<2.0	2.1	89	863	84	8.65	flowing well
SE-26-02-14	25	9.5	800	2.2	8.5	8.0	0.1	2600	890	3.6	105	933	36	8.37	pumped well
NW-28-02-13	26	13.6	1400	2.9	3.2	6.4	0.1	4900	2100	1.3	60	869	48	8.41	pumped well
SE-35-03-12	27	10.7	510	0.9	0.7	1.7	0.2	1400	10	0.9	295	756	84	8.87	pumped well
NW-33-03-11	28	10.5	380	0.7	0.3	0.9	0.2	1000	82	0.5	36	683	102	8.98	pumped well
NW-09-03-07	29	--	400	1.0	0.4	0.9	0.1	960	4.9	1.1	78	--	--	--	pumped well

Table B-1--Continued

Location (¼S,S,T,R,)	Sample Number	Temperature (°C)	Sodium (Na)	Potassium (K)	Magnesium (Mg)	Calcium (Ca)	Iron (Fe)	Total Dissolved Solids	Sulfate (SO_4)	Fluorinee (F)	Chlorine (Cl)	Bicarbonate (HCO_3)	Carbonate (CO_3)	pH	Remarks
NW-22-08-14	30	11.5	980	2.5	1.4	3.0	0.1	2600	2.8	3.1	628	1342	66	8.32	pumped well
NE-13-07-14	31	15.0	690	1.6	2.1	3.2	0.1	1900	12	7.6	292	1177	108	8.46	pumped well
NW-27-05-14	32	10.0	580	1.2	0.5	1.3	0.1	1600	7.5	4.8	114	1086	126	8.74	flowing well
NE-22-06-13	33	12.2	660	1.5	0.7	1.6	0.1	1700	4.6	7.6	227	--	--	--	pumped well
SE-23-06-10	34	11.0	430	1.4	0.5	1.5	0.2	1100	4.2	1.1	110	817	90	8.93	
NW-12-05-09	35	9.0	640	1.1	1.4	3.2	0.7	1800	140	3.2	251	891	96	8.43	pumped well
NW-10-04-08	36	10.6	390	0.9	0.4	1.0	0.1	1100	35	0.9	522	--	--	--	flowing well, may not penetrate Milk River sandstone
SE-08-02-13	38	--	5.1	0.7	7.5	19	1.6	4800	16	0.1	1.2	--	--	--	sample from Milk River
SE-23-01-11	41	13.0	570	1.2	0.8	2.5	0.1	5300	430	0.2	6.7	537	54	8.83	flowing well
SW-28-02-10	42	9.5	470	1.1	0.7	1.5	0.1	5500	310	0.4	15.7	586	96	8.74	flowing well
SE-03-05-11	43	9.0	770	2.1	1.7	4.4	1.0	4200	4.0	2.0	420	854	66	8.88	pumped well
SE-21-07-10	44	11.5	450	1.2	0.4	1.2	0.1	1200	4.0	2.8	113	817	96	8.75	flowing well
SW-19-37-09	45	8.3	320	2.9	22.0	39	2.0	2500	360	0.2	2.4	525	0	7.46	flowing well
SW-02-37-01	46	13.0	3.7	1.0	7.5	32	--	170	39	0.2	0.3	--	--	--	sample from Deer Creek

Table B-2. Nuclide concentrations for sample from southeastern Alberta and northern Montana

Sample Number	$\delta^{13}C$ (°/$_{oo}$PDB)	^{14}C (% modern)	δD (°/$_{oo}$SMOW)	$\delta^{18}O$ (°/$_{oo}$SMOW)
1	--	--	-84	-8.5
2	--	--	-67	-9.0
4	--	--	-65	-7.9
5	--	--	-73	-9.5
6	--	--	-87	-12.6
7	--	--	-95	-14.3
8	-2.7	0.0±0.6	-106	-16.0
9	--	--	-98	-11.3
10	--	--	-70	-9.0
11	-5.2	1.1±0.5	-76	-10.5
12	--	--	-98	-15.2
13	--	--	-127	-15.9
14	+2.9	0.8±0.6	-113	-16.8
15	--	--	-112	-16.6
16	--	--	-126	-16.9
17	--	--	-84	-9.5
18	--	--	-79	-9.6
19	+2.9	1.0±0.5	-90	-10.9
20	--	--	-91	-11.5
21	--	--	-101	-13.3
22	--	--	-119	-17.6

Table B-2. Continued

Sample Number	$\delta^{13}C$ (°/$_{oo}$PDB)	^{14}C (% modern)	δD (°/$_{oo}$SMOW)	$\delta^{18}O$ (°/$_{oo}$SMOW)
23	-7.8	1.6±0.4	-109	-15.1
25	+2.7	8.4±0.5	-150	-18.5
26	--	--	-157	-19.2
27	--	--	-132	-17.6
28	--	--	-132	-13.0
29	--	--	-142	-18.5
30	+1.5	0.6±0.8	--	--
31	--	--	-102	-10.7
32	-3.7	0.8±0.6	-121	-16.8
33	--	--	-97	-13.6
34	--	--	-139	-17.8
35	--	--	-128	-17.7
36	-1.7	1.4±0.5	-140	-18.7
38	--	--	--	--
41	-13.4	7.5±0.6	-141	-19.2
42	-13.7	1.6±0.1	-145	-18.6
43	--	--	-122	-15.5
44	--	--	--	--
45	-12.6	25.9±0.5	-138	-18.9

APPENDIX C

INPUT PARAMETERS TO THE GROUND-WATER FLOW MODEL

The input parameters used in the steady-state ground-water flow model WADAMO came from many sources. In all, nine parameters had to be assigned to each node: thickness, porosity, and horizontal permeability of the central aquifer (Milk River sandstone), thickness and vertical permeability of the aquitard above the central aquifer, thickness and permeability of the aquitard below the central aquifer, potentiometric head in zone overlying the three-layer system, and potentiometric head in the zone below the three-layer system. In addition, constant fluxes or constant heads were assigned to all boundary nodes and some interior nodes. The following is a discussion of the sources of these input parameters, the data density, and the reliability of each.

Milk River Sandstone Parameters

The work of Meyboom (1960) was relied on for much to the description of the central aquifer. Porosity of the Milk River sandstone was assigned a value of 10 percent based on his work. His reported values for the transmissivity (see fig. 8) for the aquifer were used in in determination of horizontal permeabilities (see section on hydrology in this thesis). Thickness of the sandstone unit (see fig. 8) was determined from interpretations of about 40 gamma and spontaneous potential

geophysical logs of oil wells throughout the study area. These logs were obtained from International Petrodata Ltd., Calgary, Alberta, Canada. Depth and locations of the wells are listed in Table C-1. Meyboom (1960) does not state the source of his porosity values, so it is difficult to evaluate the validity of such values or of the data density used in the determination. Values for transmissivity were determined by 45 field tests on wells, which ranged in duration from 10 to 720 minutes. These tests were concentrated in the central portion of the study area. There are few or no data in the southernmost part of the study area or in the northeastern corner. The areal distribution of horizontal permeabilities was mapped by dividing a representative value of transmissivity for each grid node by the thickness of the sandstone.

Aquitard Parameters

The thicknesses of the confining beds above and below the Milk River sandstone were determined from geophysical logs of oil wells. Thicknesses of the lower confining bed were plotted on a map and contoured (see fig. 30). The thickness of this shale unit showed little areal variation throughout the study area. The geophysical logs that were used typically began at depths of 300 to 600 feet below land surface. It was therefore not possible to accurately choose the thickness of the aquitard above the Milk River sandstone. The aquitard thickness was therefore estimated by assuming that it extended from the top of the Milk River sandstone to 100 feet below land surface. Borneuf's (1976) map of the hydrology of the Foremost area shows that 100 feet is a reasonable estimate of the thickness of the surficial deposits overlying the shale beds.

Table C-1. Thicknesses of aquitards and sandstone aquifer based on interpretation of geophysical logs. -- Geophysical logs were obtained from International Petrodata Ltd., Calgary, Alberta, Canada

Location of Wells[1] (sec., T., R.)	Depth of Top of Milk River Sandstone	Thickness of Upper Aquitard[2]	Depth of Bottom of Milk River Sandstone	Thickness of Sandstone	Depth of Top of Bow Island Sandstone	Thickness of Lower Aquitard
29-5-19	965	765	1080	60	2415	1335
34-4-18	750	550	860	96	2220	1362
2-6-17	750	550	900	105	2220	1320
12-12-14	1050	850	1170	68	2660	1490
29-11-18	1085	885	1200	70	2695	1495
12-12-17	835	635	980	92	2460	1480
28-1-9	790	590	930	105	2255	1325
10-1-8	960	760	1090	--	2450	1360
20-4-16	695	495	850	--	2175	1325
35-5-15	630	430	740	110	2110	1370
23-5-14	560	360	710	130	2065	1355
10-6-13	655	455	840	115	2205	1365
30-5-12	670	470	855	100	2125	1270

Table C-1. Thicknesses of aquitards and sandstone aquifer--Continued

Location of Wells[1] (sec., T., R.)	Depth of Top of Milk River Sandstone	Thickness of Upper Aquitard[2]	Depth of Bottom of Milk River Sandstone	Thickness of Sandstone	Depth of Top of Bow Island Sandstone	Thickness of Lower Aquitard
28-5-11	650	450	810	135	2100	1290
4-5-10	610	400	800	155	2120	1320
28-5-9	620	420	830	135	2115	1285
21-8-18	915	715	1050	105	2450	1400
17-9-17	745	545	870	--	2290	1420
29-8-16	710	510	860	83	2260	1400
11-10-15	625	425	830	90	2240	1410
5-10-14	660	460	765	70	2240	1475
18-10-12	590	390	750	80	2110	1460
22-8-11	625	425	755	115	2115	1360
25-10-16	--	--	750	--	2220	1470
27-11-14	--	--	770	--	2190	1420
35-10-13	660	460	840	--	2230	1390
27-11-10	865	665	1030	--	2315	1285

Table C-1. Thicknesses of aquitards and sandstone aquifer--Continued

Location of Wells[1] (sec., T., R.)	Depth of Top of Milk River Sandstone	Thickness of Upper Aquitard[2]	Depth of Bottom of Milk River Sandstone	Thickness of Sandstone	Depth of Top of Bow Island Sandstone	Thickness of Lower Aquitard
6-12-9	920	720	1110	70	2365	1255
10-3-11	--	--	690	--	1990	1300
29-4-10	645	445	810	100	2110	1300
28-5-11	650	450	800	135	2110	1310
25-6-12	560	360	720	130	2160	1340
32-9-11	590	390	730	90	2120	1390

1. All locations are west of the 4th meridian.

2. Most wells were not logged at depths shallower than 600 feet; the upper confining bed was assumed to extend upward to 100 feet below land surface.

Vertical permeabilities overlying and underlying the Milk River aquifer have not been reported in the literature. The model was run at several vertical permeabilities and the values that gave the best results were assumed to be correct. The upper shale confining bed is closer to the land surface and has been subjected to compaction and release by glaciers over the past several millions years. The loading and unloading of the shallow shales can be accompanied by fracturing. Because of the possible fracturing and because the shallow shales contain more sand than the deeper confining bed, the vertical permeability of the upper shale was assumed to be twice the vertical permeability of the lower shales. The permeabilities that gave the best results in the model were 5.0×10^{-7} and 2.5×10^{-7} gpd/ft^2 in the overlying and underlying confining beds, respectively.

Potentiometric Surface above Upper Confining Beds

The unconfined aquifer in the eastern half of the study area has been previously mapped by Borneuf (1976). This map has been incorporated into a water-table map (fig. 7) for the entire study area. The water-table contours for the remaining area were determined by contouring surface-water elevations as shown on Canadian Department of Energy, Mines, and Resources topography maps for Foremost, Alberta (1968) and Lethebridge, Alberta (1967). Water-table contours, as determined by this method, were generally about 50 feet below the land surface. This value agrees well with water levels in surficial deposits reported by Borneuf (1976).

Potentiometric Surface below Lower Confining Bed

The Bow Island formation is the next continuous sandstone below the Milk River aquifer and is separated from it by about 1,300 to 1,500 feet of clays and shales. The potentiometric surface of the Bow Island formation was mapped by Schwartz and Muehlenbachs (1980) based on analyses of 161 drill-stem tests. The Bow Island formation has been heavily developed for oil and gas. The impacts of this development are expressed on the Schartz and Muehlenbachs map as drawndown cones around the larger gas and oil fields. Figure 11 shows the potentiometric surface of the Bow Island formation that has been generalized to neglect the effects of the oil and gas development; it was generalized after figure 2 of Schwartz and Muehlenbachs (1980).

Constant Fluxes

All nodes along the northern boundary and most nodes on the eastern and western boundaries of the grid were assigned constant flux values. The flux in the Milk River aquifer across the northern boundary was assumed to have remained nearly the same since prior to downcutting of the Milk River. The great distance between the northern boundary and the Milk River (about 50 miles) and the low transmissivities (10 to 20 gpd/ft) in the region of the northern boundary would provide support for this assumption. The flux across the northern boundary was calculated by using the standard value of transmissivity of the Milk River sandstone and the northward component of the hydraulic gradient at each node and applying Darcy's law. Although the fluxes varied from node to node, most were in the range of 2 to 3

gpd for each node. Each node represented an area 7,000 to 10,000 feet wide.

The initial east and west boundary fluxes were assigned values of zero, which caused the contours on the modeled steady-state potentiometric surface to be perpendicular to these boundaries. The model yielded potentiometric surface contours that trended east-west at the eastern and western grid boundaries and northeast-southwest through the center of the model grid, indicating that the zero flux boundaries were artificially constraining the direction of flow in the aquifer. The east and west boundary fluxes were therefore adjusted so that the trend of the contour in the center was continued to the grid edge.

Constant Heads

Constant head values were assigned to nodes that approximated the locations of the Milk River sandstone outcrop in the study area. Head values were taken from ponded surface-water elevations in the areas of the outcrop based on land-surface topography map published by the U.S. Geological Survey for Montana and the Department of Energy, Mines, and Resources for Alberta. The present-day potentiometric surface of the Milk River aquifer indicates that the areas of sandstone outcrop are the recharge areas to the aquifer.

REFERENCES

Bentley, Harold. 1982. Personal communication. Assistant Research Professor, Department of Hydrology and Water Resources, University of Arizona, Tucson

Barker, J. F., P. Fritz, and R. M. Brown. 1978. Carbon-14 measurements in aquifers with methane. In Isotope techniques in Groundwater Hydrology, 1978. (Proceedings from a symposium in Vienna, 1978). IAEA, Vienna, 661-678.

Borneuf, D. M. 1976. Hydrogeology of the Foremost area, Alberta. Alberta Res. Council Rept. 74-4.

Brinkman, J. E. 1982. Water age dating of the Carrizo sand. Unpublished M.S. thesis, University of Arizona, Tucson.

Clayton, R. N., I. Freidman, D. L. Graf, T. K. Mayeda, W. F. Meents, and N. F. Shimp. 1965. The origin of saline formation waters. I. Isotopic composition. Jour. Geophys. Res., 71, 3869-3882.

Coplen, T. B., and B. B. Hanshaw. 1973. Ultrafiltration by a compacted clay membrane. I. Oxygen and hydrogen isotopic fractionation. Geochem. Cosmochem. Acta, 37, 2295-2310.

Craig, H. 1961. Isotopic variations in meteoric waters. Science, 133, 1702-1703.

Crockford, M. B. B. 1949. Oldman and Foremost formations of southern Alberta. Am. Assoc. Petroleum Geologists Bull., 33, 500-510.

Dansgaard, W. 1964. Stable isotopes in precipitation. Tellus, 16, 436-468.

Davis, S. N. 1969. Porosity and permeability of natural materials. In DeWiest, R. J. M., ed., Flow through Porous Media. Academic Press, New York, 54-89.

Davis, S. N., and R. J. M. De Wiest. 1967. Hydrogeology. John Wiley and Sons, New York, 463 pp.

Deines, P., D. Langmuir, and R. S. Harmon. 1974. Stable carbon isotope ratios and the existence of a gas phase in the evolution of carbonate ground waters. Geochem. Cosmochem. Acta, 38, 1147-1164.

Englehardt, W. V., and K. H. Gaida. 1963. Concentration changes of pore solutions during the compaction of clay sediments. Jour. Sed. Petrology, 33, 919-930.

Flint, R. F. 1971. Glacial and Quaternary Geology. John Wiley and Sons, Inc., New York, 882 pp.

Fontes, J. C., and J. M. Garnier. 1979. Determination of the initial ^{14}C activity of the total dissolved carbon: A review of the existing models and a new approach. Water Resources Res., 15, 399-413.

Freeze, R. A., and J. A. Cherry. 1979. Groundwater. Prentiss-Hall, Inc., Englewood Cliffs, New Jersey, 604 pp.

Graf, D. L., I. Freidman, and W. F. Meents. 1965. The origin of saline formation waters. II. Isotopic fractionation by shale micropore systems. Illinois State Geol. Survey Circ. 393.

Gravinor, A. P., and L. A. Bayrock. 1965. Glacial deposits of Alberta. In Soils in Canada. Royal Soc. Canada Spec. Publ. 3, 33-50.

Heusser, C. J. 1977. Quaternary palynology of the Pacific slope of Washington. Quaternary Res., 8, 282-306.

Hoefs, J. 1980. Stable Isotope Geochemistry. Springer-Verlag, Berlin, 208 pp.

Hitchon, B., and I. Freidman. 1969. Geochemistry and origin of formation waters in the western Canada sedimentary basin. I. Stable isotopes of hydrogen and oxygen. Geochem. Cosmochem. Acta, 33, 1321-1349.

Kemp, J. E., and P. Billingsley. 1921. Sweet Grass Hills, Montana. Geol. Survey America Bull., 32, 437-478.

Kharaka, Y. K., and F. A. F. Berry. 1974. The influence of geological membranes on geochemistry of subsurface waters from Miocene sediments at Kettleman North Dome of California. Water Resources Res, 10, 313-327.

Meijer-Drees, M. C. 1973. The Milk River formation in the Suffield and Medicine Hat areas, Alberta. Canada Geol. Survey Paper 73-1, Part B, 189-191.

Meyboom, P. 1960. Geology and groundwater resources of the Milk River sandstone in southern Alberta. Albert Res. Council Mem. 2.

Pearson, F. J., and B. B. Hanshaw. 1970. Sources of dissolved carbonate species in ground water and their effects on carbon-14 dating. Isotope Hydrology, IAEA, Vienna, 271-286.

Phillips, F. M. 1980. Possible effects of ion filtration on ^{36}Cl and other ground-water tracers. Preliminary manuscript, Department of Geosciences, University of Arizona, Tucson.

Piper, A. M. 1944. A graphic procedure in the geochemical interpretation of water analysis. Trans. Geophys. Union Trans, 2, 914-923.

Plummer, L. N. 1977. Defining reactions and mass transfer in part of the Floridan aquifer. Water Resources Res., 13, 801-802.

Russell, L. S., and R. W. Landes. 1940. Geology of the southern Alberta plains. Canada Dept. Mines Res., Geol. Survey Mem. 221.

Schwartz, F. W., and K. Muehlenbachs. 1979. Isotope and ion geochemistry of groundwaters in the Milk River aquifer, Alberta. Water Resources Res., 15, 259-269.

_____ 1980. Chemical evolution of formation waters in a sedimentary basin. Extended abstract from the International Conference on Rock-water Interaction, Edmonton, Alberta.

Schoell, M. 1980. The hydrogen and carbon compositions of methane from natural gases of various origins. Geochem. Cosmochem. Acta, 4, 649-661.

Stumm, W., and J. J. Morgon. 1970. Aquatic Chemistry. John Wiley and Sons, New York, 583 pp.

Tamers, M. A., 1975. Validity of radiocarbon dates on groundwater. Geophys. Surv., 2, 217-239.

Taylor, R. S., W. H. Mathews, and W. O. Kupsch. 1964. Tertiary. In Alberta Society of Peteroleum Geologists, ed., Geological History of Western Canada, 190-194.

Thorstenson, D. C., D. W. Fisher, and M. G. Croft. 1979. The geochemistry of the Fox Hills–Basal Hell Creek aquifer in southwestern North Dakota and northwestern South Dakota. Water Resources Res., 15, 1479-1498.

Winograd, I. J., and G. M. Farlekas. 1974. Problems in ^{14}C dating of water from aquifers of deltaic origin. In Isotope Techniques in Groundwater Hydrology 1974. (Proceedings from a symposium in Vienna, 1974). IAEA, Vienna, 69-93.

Williams, G. D., and C. F. Burk. 1964. Upper Cretaceous. In Geological History of Western Canada. Alberta Society of Petroleum Geologists, 169-189.

Van Donk, J. 1976. ^{18}O record of the Atlantic Ocean for the entire Pleistocene Epoch. Geol. Soc. America Mem. 145, pp. 147-163.

Young, A., P. F. Low, and A. S. McLatchie. 1964. Permeability studies of argillaceous rocks. Jour. Geophys. Res., 69, 4237-4245.